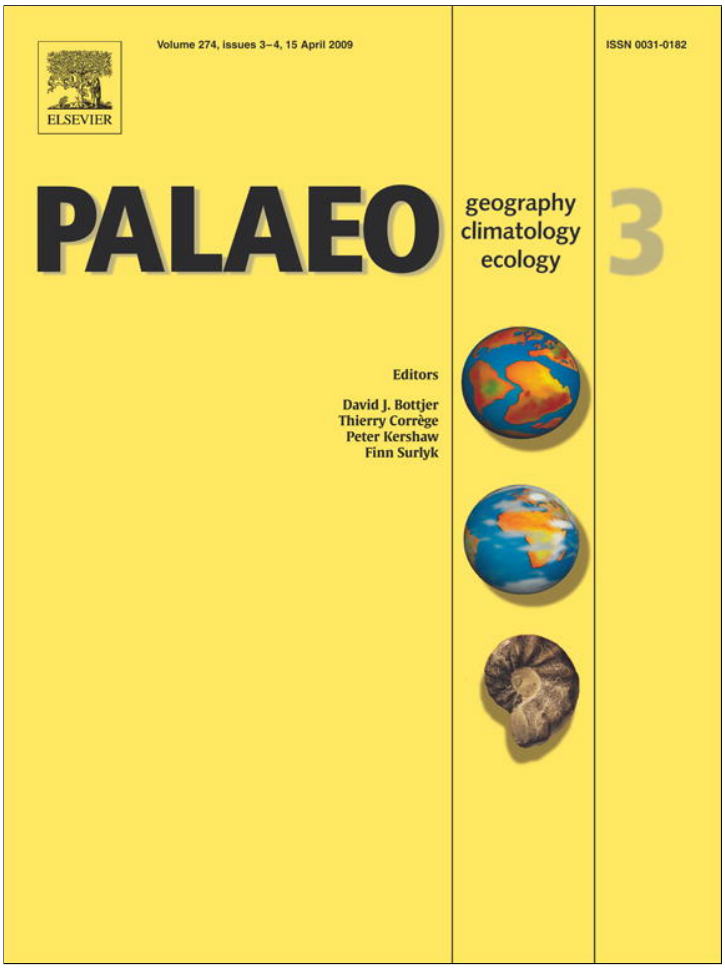

Palaeogeography, Palaeoclimatology, Palaeoecology 274 (2009) 140–159

Contents lists available at ScienceDirect

Palaeogeography, Palaeoclimatology, Palaeoecology

journal homepage: www.elsevier.com/locate/palaeo

Early history of the Western Pacific Warm Pool during the middle to late Miocene (~13.2–5.8 Ma): Role of sea-level change and implications for equatorial circulation

Stephen A. Nathan, R. Mark Leckie *

Department of Geosciences, University of Massachusetts, Amherst, Massachusetts, 01003 USA

ARTICLE INFO

Article history:
Received 21 August 2007
Received in revised form 13 January 2009
Accepted 19 January 2009

Keywords:
Western Pacific Warm Pool
Carbonate crash
Biogenic bloom
Equatorial Pacific
Indonesian Seaway
Planktic foraminiferal isotope paleoecology
Middle to late Miocene
Mi events
Sea level
Ocean circulation
Central American Seaway

ABSTRACT

We document the waxing and waning of a "proto-warm pool" in the western equatorial Pacific (WEP) based on a study of multi-species planktic foraminiferal isotope ratios and census data spanning the 13.2–5.8 Ma interval at ODP Site 806. We hypothesize that the presence or absence of a proto-warm pool in the WEP, caused by the progressive tectonic constriction of the Indonesian Seaway and modulated by sea level fluctuations, created El Niño/La Niña-like alternations of hydrographic conditions across the equatorial Pacific during the late Miocene. This hypothesis is supported by the general antithetical relationship observed between carbonate productivity and preservation in the western and eastern equatorial Pacific, which we propose is caused by these alternating ocean–climate states. Warming of thermocline and surface waters, as well as a major change in planktic foraminferal assemblages record a two-step phase of proto-warm pool development ~11.6–10 Ma, which coincides with Miocene isotope events Mi5 and Mi6, and sea-level low stands. We suggest that these changes in the biota and structure of the upper water column in the WEP mark the initiation of a more modern equatorial current system, including the development of the Equatorial Undercurrent (EUC), as La Niña-like conditions became established across the tropical Pacific. This situation sustained carbonate and silica productivity in the eastern equatorial Pacific (EEP) at a time when carbonate preservation sharply declined in the Caribbean. Proto-warm pool weakening after ~10 Ma may have contributed to the nadir of a similar "carbonate crash" in the EEP. Cooling of the thermocline and increased abundances of thermocline taxa herald the decay of the proto-warm pool and higher productivity in the WEP, particularly ~9.0–8.8 Ma coincident with a major perturbation in tropical nannofossil assemblages. We suggest that this interval of increased productivity records El Niño-like conditions across the tropical Pacific and the initial phase of the widespread "biogenic bloom". Resurgence of a later proto-warm pool in the WEP ~6.5–6.1 Ma may have spurred renewed La Niña-like conditions, which contributed to a strong late phase of the "biogenic bloom" in the EEP.

1. Introduction

The opening and closing of ocean gateways have played a major role in the evolution of Cenozoic ocean circulation and the distribution of heat and salt, which in turn have impacted global climate and marine primary productivity (e.g., Berggren and Hollister, 1977; Kennett, 1977; Keigwin, 1982; Covey and Barron, 1988; Mikolajewicz et al., 1993; Raymo, 1994; Heinze and Crowley, 1997; Haug and Tiedemann, 1998; Kameo and Sato, 2000; Nisancioglu et al., 2003; Schneider and Schmittner, 2006). A number of studies have demonstrated that there were major changes in equatorial Pacific circulation during the middle to late Miocene due to the gradual constriction of the Indonesian Seaway (e.g., van Andel et al., 1975; Srinivasan and Kennett, 1981; Keller, 1985; Kennett et al., 1985; Romine and Lombari, 1985; Savin et al., 1985; Theyer et al., 1989; Gasperi and Kennett, 1992, 1993a,b; Hodell and Vayavananda, 1993; Norris et al., 1993; Kuhnt et al., 2004). The development of the Western Pacific Warm Pool (WPWP), or a "proto-warm pool", is a consequence of the gradual constriction ("closure") of the Indonesian Seaway as the Australian Plate collided with Southeast Asia. Evidence for the existence of a proto-warm pool should be a pronounced west to east thermocline gradient across the equatorial Pacific (i.e., thermocline tilt; deep in the west and shallow in the east), accompanied by a strong west to east productivity gradient (weak in the west and strong in the east) (e.g., Ravelo et al., 2006). The purpose of this project was to better constrain the early history of the WPWP and to consider this history in the context of the equatorial current system and tropical climate during the late Miocene.

To investigate the early history of a proto-warm pool in the western equatorial Pacific (WEP), deep-sea sediment samples were obtained from Ocean Drilling Program (ODP) Site 806 on the Ontong Java Plateau, located in the center of the present-day WPWP (Fig. 1). The Ontong Java Plateau is a broad oceanic plateau that straddles the

* Corresponding author. Tel.: +1 413 545 1948.
E-mail address: mleckie@geo.umass.edu (R.M. Leckie).

0031-0182/$ – see front matter © 2009 Elsevier B.V. All rights reserved.
doi:10.1016/j.palaeo.2009.01.007

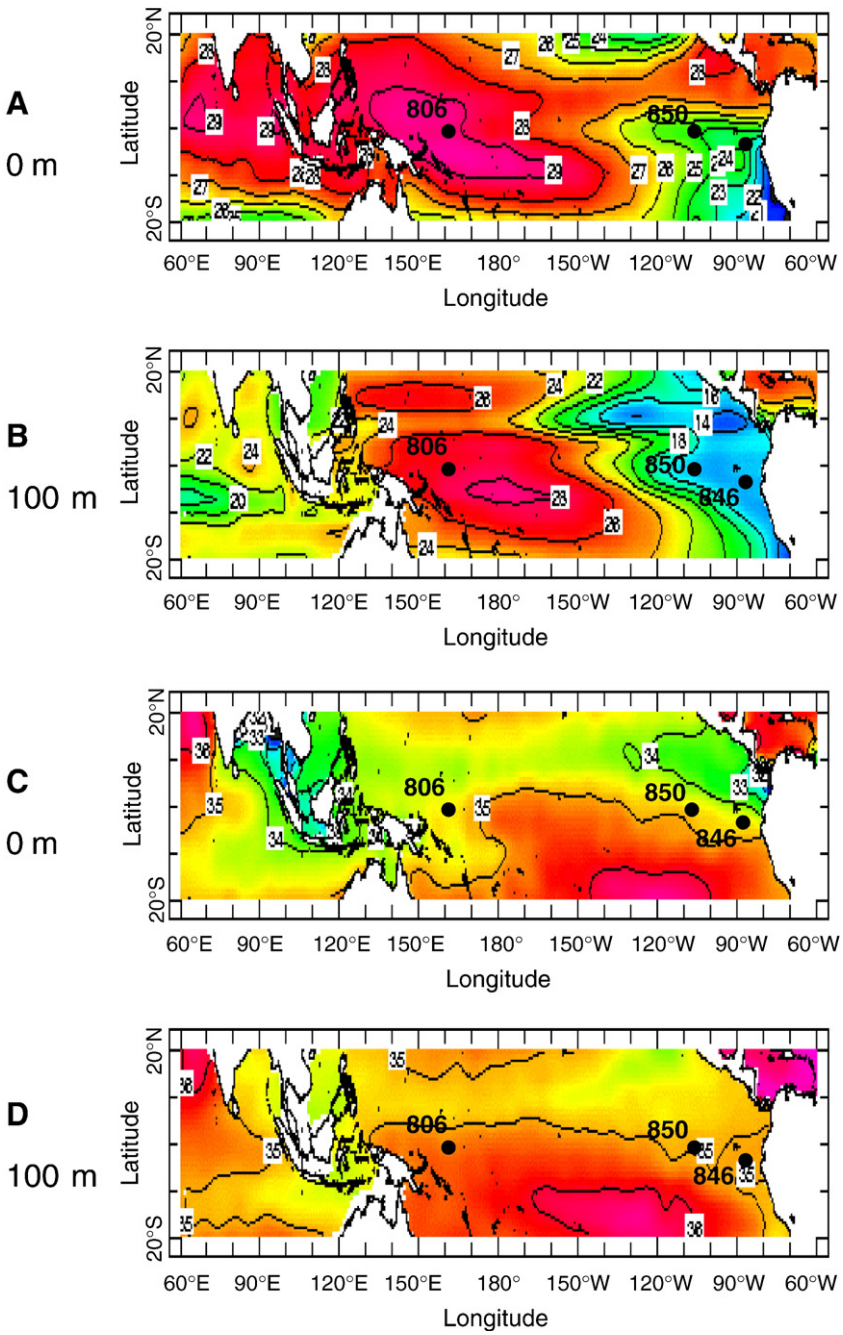

Fig. 1. Mean annual temperature at the sea surface (panel A) and 100 m water depth (panel B; Levitus and Boyer, 1994), and salinity at the sea surface (panel C) and at 100 m water depth (panel D; Levitus et al., 1994) across the tropical Pacific. The locations of ODP Site 806 in the western equatorial Pacific (primary study site), and Sites 846 and 850 in the eastern equatorial Pacific (discussed in text) are labeled. Site 806 is located in the core of the present-day Western Pacific Warm Pool.

Equator. It is isolated from terrigenous input from landmasses to the west and south. Site 806 has been within 1° of the equator for the past 15 million years, and it may have crossed the Equator between 15 Ma and 10 Ma (Acton pers. comm., 2005; based on an updated reconstruction of Acton, 1999). Therefore, Site 806 has been in an ideal position to record changes in the upper water column of the WEP since the late Miocene. To characterize such changes through time, we collected multi-species isotope ratios and planktic foraminifer population census data. The results presented here build on earlier research (e.g., Kennett et al., 1985; Keller, 1985; Gasperi and Kennett, 1993a; Hodell and Vayavananda, 1993; Li et al., 2006). We have also compared our findings with published data from the eastern equatorial Pacific (EEP) in order to gain a better understanding of how equatorial Pacific circulation and climate evolved as both the Indonesian and Central American seaways became increasingly constricted during the middle and late Miocene (e.g., Farrell et al., 1995b; Lyle et al., 1995; Droxler et al., 1998; Roth et al., 2000; Kameo and Sato, 2000) (Fig. 1).

2. Background

The gradual closure of the Indonesian Seaway during the Neogene had a major impact on equatorial circulation with the formation of the Western Pacific Warm Pool (WPWP) and development of the

Equatorial Undercurrent (EUC). Changes in foraminiferal and radiolarian assemblages in the early late Miocene were interpreted as recording the "closure" of the Indonesian Seaway and establishment of a modern equatorial Pacific circulation, including development of the Equatorial Countercurrent and EUC (Kennett et al., 1985; Romine and Lombari, 1985). Subsequent isotopic studies have supported this interpretation (e.g., Gasperi and Kennett, 1993a,b; Hodell and Vayavananda, 1993). However, the timing of the tectonic constriction of the Indonesian Seaway has remained poorly constrained, with estimates ranging from ~17 to 3–4 Ma (e.g., Kennett et al., 1985; Hodell and Vayavananda, 1993; Nishimura and Suparka, 1997; Srinivasan and Sinha, 1998; Jian et al., 2006; Li et al., 2006). Modeling studies have suggested that the WPWP formed during the Pliocene after New Guinea drifted far enough north to effectively block warm, saline South Pacific water from being transported into the Indian Ocean (Cane and Molnar, 2001; Molnar and Cane, 2002). Foraminiferal assemblages and multi-species isotopic analyses from deep-sea cores spanning the equatorial Pacific also show the evolution of the modern WPWP and circulation after ~3.6–3.0 Ma in the Pliocene (Chaisson, 1995; Cannariato and Ravelo, 1997; Chaisson and Ravelo, 2000; Ravelo et al., 2006; Sato et al., 2008).

Also unknown are the effects that Indonesian Seaway constriction and warm pool development may have played in the early late Miocene "carbonate crash" (an anomalous decrease of carbonate in deep sea sediments) and the late Miocene "biogenic bloom" (a sharp increase in carbonate accumulation rates across the tropical Indo-Pacific) (van Andel, 1975; Vincent et al., 1981; Keller and Barron, 1983; Peterson et al., 1992; Berger et al., 1993; Farrell et al., 1995b). The "carbonate crash" of the eastern equatorial Pacific (EEP; ~11–9 Ma) and its precursor event in the Caribbean (~12–10 Ma) have been attributed to: 1) a reorganization of deep-water circulation due to the tectonic constriction of the Central American Seaway; 2) a rise of the carbonate compensation depth (CCD); and 3) low carbonate productivity (Farrell et al., 1995b; Lyle et al., 1995; Sigurdsson et al., 1997; Droxler et al., 1998; Roth et al., 2000; Lyle, 2003; Jiang et al., 2007; Newkirk and Martin, 2009). On the other hand, the late Miocene–early Pliocene "biogenic bloom" has been attributed to increased biological productivity stimulated by increased nutrient delivery to the world ocean as a consequence of increased continental weathering rates associated with the uplift of Himalaya–Tibetan Plateau and Andes (e.g., Hodell et al., 1991; Filippelli and Delaney, 1994; Pisias et al., 1995; Filippelli, 1997; Martin et al., 1999; Hermoyian and Owen, 2001; Diester-Haass et al., 2005). Phosphorous mass accumulation rates suggest that increased nutrient delivery occurred in two pulses with one peak at ~9.0 Ma, and a second stronger peak centered at 6.5–4.0 Ma (Hermoyian and Owen, 2001). Reorganization of deep water circulation has also been proposed as the primary cause of increased nutrient delivery to the Indo-Pacific that sustained this widespread episode of elevated productivity (e.g., Dickens and Owen, 1999; Grant and Dickens, 2002). What are the causal relationships, if any, between the closure history of the Indonesian Seaway and these widespread changes in tropical carbonate production and preservation?

Unlike the Central American Seaway, the modern day Indonesian Seaway is not completely closed. Instead, the Indonesian Throughflow (ITF) between Borneo and New Guinea is an important pathway for the return of surface waters to the Atlantic, and it contributes to the inter-basin balance of heat, mass, and salt via the global conveyor (Gordon, 1986; Broecker, 1991; Shriver and Hurlburt, 1997; Stewart, 2005). However, the waters of the Pacific equatorial current system are constricted as they flow through the narrow passages of the Indonesian Seaway causing the waters pushed by the strong easterly Trade Winds to pile up and form the WPWP. Today, the WPWP is a thick and widespread lens of warm water, delineated by the 28 °C isotherm, that seasonally extends from the central equatorial Pacific to the eastern Indian Ocean (Yan et al., 1992; Martinez et al., 1998).

The WPWP is a major a component of the equatorial current system, the El Niño-Southern Oscillation (ENSO), and it contributes to the diabatic heating of the tropical atmosphere, affecting both the Hadley and Walker Circulations (McPhaden and Picaut, 1990; Webster, 1994). The mixed layer of the western equatorial Pacific is thick and seasonably stable with a depressed but strong thermocline, which shoals toward the east creating the observed west–east asymmetry in upper water column hydrography and productivity. The westward winds in the tropics cause surface waters to pile up in the WEP, which creates an eastward pressure force (Philander, 1980; Stewart, 2005). Some of the water that piles up in the WPWP flows eastward as a narrow jet 50–250 m below the surface at the Equator. This Equatorial Undercurrent (EUC), also known as the Cromwell Current, delivers nutrient-rich thermocline waters to the central and eastern equatorial Pacific where the mixed layer is thinner and the thermocline shoals high into the photic zone due in part to Coriolis-driven divergence at the equator (e.g., Tomczak and Godfrey, 1994; Wells et al., 1999; Goodman et al., 2005; Ziegler et al., 2007). The upper water column structure at the location of Site 806 was likely influenced by the doming of isotherms in the thermocline due to the influence of the EUC at times when the WPWP, or proto-warm pool, was present (Hodell and Vayavananda, 1993; Stewart, 2005) owing to the location of this site at or very near the equator.

It is now generally accepted that the modern west–east asymmetry in equatorial thermocline structure, sea surface temperatures, and productivity became established after 3.6 or 3.0 Ma (Chaisson, 1995; Cannariato and Ravelo, 1997; Chaisson and Ravelo, 2000; Molnar and Cane, 2002; Ravelo et al., 2004, 2006; Sato et al., 2008). Prior to this, the early Pliocene warm period (~4.5–3.0 Ma) was characterized by a long-term El Niño-like state (Molnar and Cane, 2002; Wara et al., 2005; Ravelo et al., 2006). Were El Niño-like conditions the norm during the middle and late Miocene as well? How might tectonic gateway constriction in the western tropical Pacific have influenced wind-driven ocean circulation and climate during the middle to late Miocene? Finally, did the WPWP and EUC develop during the late Miocene? This study provides some preliminary answers to these questions.

3. Methods

3.1. Planktic foraminiferal assemblages and multi-species isotopic analyses

Continuous sediment samples from ODP Site 806 (2520 m water depth, 0°19.1′N, 159°21.7′E) were analyzed at a resolution of ~64 kyr ($1\sigma = 33$ kyr) through the study interval (13.2–5.8 Ma). Samples were disaggregated by soaking the sediment in a mixture of water, hydrogen peroxide, and Calgon for at least 24 h. The mixture was then washed over a 63-μm screen and the residues were dried in an oven at 60 °C.

In order to understand the paleoecology of ancient species of planktic foraminifera, including many extinct taxa (nearly 75% of the species analyzed are now extinct), we first conducted detailed multi-species, multi-discrete size fraction analyses of four representative samples through the study interval (time slices at 7.30 Ma, 8.90 Ma, 10.53 Ma, and 12.99 Ma), plus a box core sample from Ontong Java Plateau that provided a modern baseline for the extant taxa (Nathan, 2005). The purpose of these analyses was to establish ontogenetic trends and depth ranking (e.g., Berger et al., 1978). This study also tested whether extant species behaved in similar ways >5 million years ago. These analyses allowed us to: 1) assign an extinct species to a particular water layer; 2) test previously published water layer assignments; and 3) record changes in a species depth habitat during ontogeny.

For the planktic foraminiferal assemblage time series, a minimum of 300 planktic foraminifer tests of the >150 μm size fraction were identified and counted. Counts for each sample were then binned as mixed layer assemblage 1, mixed layer assemblage 2, thermocline assemblage 1, thermocline assemblage 2, and "other species" based on

our species-specific isotope paleoecologic analysis described below. Dissolution was gauged by counting test fragments. Benthic foraminifers, radiolarians, mineral fragments, and other particles were also counted.

Today, mixed layer taxa *Globigerinoides* spp. and *Globigerinita glutinata* dominate the sediment assemblages that accumulate beneath the modern WPWP (also see sediment trap studies of Yamasaki et al., 2008). These taxa are used to define Mixed Layer Assemblage 1 in our census data. Mixed Layer Assemblage 2 consists of mostly extinct species (*Paragloborotalia mayeri*, *Dentoglobigerina altispira*, *Globoturborotalita woodi*, *G. apertura*, *G. decoraperta*, *G. druryi*) plus *Globigerina bulloides*. Chaisson and Ravelo (2000) had assessed species of *Globoturborotalita* as thermocline dwellers. Our findings differ; three of the Miocene *Globoturborotalita* species yield isotope paleoecologic results indicative of a mixed layer habitat, while one species (*G. nepenthes*) has more positive δ^{18}O values indicative of the thermocline (Nathan, 2005). Thermocline Assemblage 1 consists of species of *Globorotalia* and *Neogloboquadrina* (excluding *N. continuosa*), while Thermocline Assemblage 2 consists of extinct (and dissolution resistant) species: *Globoturbolotalita nepenthes*, *Globoquadrina dehiscens*, and species of *Sphaeroidinellopsis* (*S. seminulina*, *S. kochii*, *S. subdehiscens*). The "other" category in the time series of sediment assemblages includes rare mixed layer and thermocline species.

For the isotopic time series, three planktic species and one benthic taxon were analyzed. We selected the non-saccate *Globigerinoides sacculifer* as our mixed layer (ML) proxy for the continuous record of stable isotope analyses because plankton tow and isotopic studies have shown that modern *G. sacculifer* lives relatively deep in the mixed layer (Ravelo and Fairbanks, 1992; Loncaric et al., 2006). In addition, it is a long-ranging taxon that has been used by numerous investigators as a near-surface proxy thereby allowing results of this study to be compared to other published results. Ten to twelve tests of *G. sacculifer* sensu lato were analyzed (250–300 μm size fraction; lacking the final saccate, gametogenic chamber; here probably including *G. immaturus* and *G. quadrilobatus* of Kennett and Srinivasan, 1983).

Our isotope paleoecology studies demonstrated that *Globorotalia menardii* consistently yields δ^{18}O values that indicate it lived within the upper thermocline (UTH) during the late Miocene. Today, *G. menardii* is known to occur in greatest abundances in association with the chlorophyll maximum zone, similar to *Neogloboquadrina dutertrei* (e.g., Fairbanks and Wiebe, 1980; Fairbanks et al., 1980, 1982; Ravelo and Fairbanks, 1992; Curry et al., 1983; Cannariato and Ravelo, 1997; Patrick and Thunell, 1997; Faul et al., 2000), where peak productivity is facilitated by filtered solar radiation from above and advection of nutrients from below. Therefore, its position in the upper thermocline is likely controlled by the availability of food rather than temperature per se. The 355–425 μm size fraction is used in the stable isotope time series because it is generally abundant in this size range and it minimizes ontogenetic variability. Approximately six tests of *Globorotalia menardii* were analyzed. Specimens of *Globorotalia (Fohsella) fohsi* were used in the record before ~12 Ma and *G. menardii* thereafter (three samples between ~12.0 Ma and 11.7 Ma contain both *G. (F.) fohsi* and *G. praemenardii*. At Site 806, the last occurrence (LO) of *G. (F.) fohsi* was ~11.68 Ma, and the first occurrence (FO) of *G. menardii* was ~11.65 Ma. Vincent and Toumarkine (1995) found identical orbitally-tuned ages for these two biostratigraphic datums at ODP Site 846 in the eastern equatorial Pacific. In the southern Caribbean ODP Site 999, Chaisson and D'Hondt (2000) reported the LO of *G. (F.) fohsi* in the same sample as the FO of *G. menardii*.

To represent the deep thermocline (DTH) for the isotope time series, the 355–425 μm size fraction of *Globoquadrina venezuelana* was selected because like *G. menardii*, it is long-ranging and persistent throughout the study interval at Site 806. Previous studies have recognized *G. venezuelana* as a deep thermocline dweller (e.g., Barrera et al., 1985; Keller, 1985; Vincent and Killingley, 1985; Gasperi and Kennett, 1992, 1993a,b; Corfield and Cartlidge, 1993; Hodell and Vayavananda, 1993; Norris et al., 1993; Pearson and Shackleton, 1995). Our isotope paleoecology studies demonstrate that tests of this species undergo δ^{18}O enrichment during ontogeny and that the 355–425 μm size fraction consistently represents individuals that inhabited the deeper part of the thermocline, but not as deep as subthermocline-dwelling *Globorotalia scitula*. Approximately six tests of *G. venezuelana* were analyzed for the isotope time series.

As many tests as possible of the epifaunal benthic (B) taxa *Planulina wuellerstorfi* and/or *Cibicidoides* spp. were collected to assess deep-water conditions. In the interval prior to ~9.5 Ma, *Cibicidoides* spp. were used in nearly all the analyses, while *P. wuellerstorfi* was used in most analyses younger than 9.5 Ma (Appendix 1). Ten samples through the study interval contained sufficient numbers of both taxa for isotopic analyses, and eight of these samples had little appreciable δ^{18}O difference (<0.10‰) between *Cibicidoides* spp. and *P. wuellerstorfi*; therefore, no corrections were applied to the *Cibicidoides* values.

For each isotopic analysis, foraminifer tests were crushed, sonicated, and decanted in a succession of three rinses to remove chalky residue prior to analysis. Isotope analyses were performed on every sample for which a population analysis was conducted. Stable isotope analyses were performed at the University of South Florida, College of Marine Science using a Finnigan-MAT Delta Plus XL mass spectrometer with a Kiel III automated carbonate device having an analytical precision of +/−0.08‰ for δ^{18}O and +/−0.04‰ for δ^{13}C (T. Quinn, 2002, personal communication).

Table 1
Biostratigraphic basis of revised age model for ODP Site 806, Ontong Java Plateau, western equatorial Pacific: planktic foraminifer (Chaisson and Leckie, 1993) and calcareous nannofossil (Takayama, 1993) datums from Site 806, and planktic foraminifer datums (Srinivasan and Kennett, 1981; Hodell and Vayavananda, 1993; latter in italics) from nearby DSDP Site 289.

Foram datums	Datum age	Author	806 (mbsf)	289 (mbsf)
LO *G. nepenthes*	4.39	C&P1997	111.90	114.00
FO *G. tumida*	5.82	C&P1997	172.04	167.00
FO *P. primalis*	6.40	B1995	206.15	192.00
FO *G. plesiotumida*	8.58	C&P1997	267.06	233.00
FO *N. acostaensis*	9.82	C&P1997	354.68	308.50
LO *G. mayeri*	10.49	C&P1997	364.37	335.50
FO *G. nepenthes*	11.19	C&P1997	378.00	348.00
LO *G. fohsi*	11.68	C&P1997	412.79	390.00
FO *G. fohsi*	13.42	C&P1997	449.89	434.00
Nanno datums		Datum age	Author	806 (mbsf)
LO *T. rugosus*		5.23	B&R1997	151.38
LO *D. quinqueramus*		5.59	R2006	160.88
FO *A. amplificus*		6.84	B&R1997	213.13
FO *D. berggrenii*		8.52	R2006	284.38
FO *R. pseudoumbilicus* paracme		8.85	R&F1995	310.56
LO *D. hamatus*		9.56	R2006	336.93
FO *D. hamatus*		10.54	R2006	365.28
FO *C. coalitus*		10.79	B&R1997	374.98
LO *G. fohsi* (foraminifer)		11.68	C&P1997	412.79
LO *S. heteromorphus*		13.53	R2006	475.68

LO = last occurrence, FO = first occurrence. Datum ages provided in these original publications have been updated to orbitally-tuned age models: B1995 = Berggren et al. (1995); B and R1997 = Backman and Raffi (1997); C and P1997 = Chaisson and Pearson (1997); R2006 = Raffi et al. (2006); R and F1995 = Raffi and Flores (1995). The age model used in this paper is based primarily on the calcareous nannofossil datums presented here. We also used the LO *Globorotalia (Fosella) fohsi* s.l. (planktic foraminifer) in our age model because of its consistent orbitally-tuned age and biostratigraphic position at ODP Site 846 in the eastern equatorial Pacific (ODP Leg 138; Shackleton et al., 1995; Vincent and Toumarkine, 1995) and in the western tropical Atlantic (ODP Leg 154; Chaisson and Pearson, 1997).

3.2. Age model and sedimentation history on Ontong Java Plateau

The upper middle Miocene to upper Miocene interval of ODP Site 806 is characterized by a monotonous sequence of white nannofossil ooze and chalk with varying proportions of planktic foraminifers (Kroenke et al., 1991). The original age models based on calcareous nannofossils (Takayama, 1993) and planktic foraminifers (Chaisson and Leckie, 1993) were based on the Berggren et al. (1985) time scale. Here we used the Berggren et al. (1995) time scale, supplemented with astronomically tuned calcareous nannofossil (Backman and Raffi, 1997) and planktic foraminifer (Chaisson and Pearson, 1997) datums (Table 1). Fig. 2 compares the planktic foraminiferal age-depth model for ODP Site 806 (Chaisson and Leckie, 1993), updated with the orbitally-tuned datum ages, to nearby DSDP Site 289 (Srinivasan and Kennett, 1981). The two planktic foram age models reveal a strikingly similar sedimentation history with highest sediment accumulation rates in the 11.68–11.19 Ma and 9.82–8.58 Ma intervals. The calcareous nannofossil age model shows less variability. The nannofossil age model was adopted for this study because of the more widespread use of nannofossil datums for age control and correlation in tropical paleoceanographic studies. Dry bulk density, percent carbonate (Kroenke et al., 1991), and linear sedimentation rates were used to calculate carbonate mass accumulation rates (MARs). Carbonate MARs fluctuated through the study interval from ~2.5 to ~8 g/cm^2/kyr.

3.3. Reconstructing upper water column hydrography

Today, the western equatorial Pacific is dominated by the WPWP, which is characterized by a thick mixed layer, a deep, well-developed thermocline, and a deep chlorophyll maximum (Fig. 3). Based on a box core sediment assemblage collected near ODP Site 806, this water column structure yields relatively small $\delta^{18}O$ gradients between mixed layer dwelling *G. sacculifer* and upper thermocline *G. menardii* ($\Delta\delta^{18}O_{men\text{-}sac} = 0.66‰$) and *N. dutertrei* ($\Delta\delta^{18}O_{dut\text{-}sac} = 0.82‰$), as well as deeper thermocline *G. tumida* ($\Delta\delta^{18}O_{tum\text{-}sac} = 1.20‰$) (Table 2). Ravelo and Fairbanks (1992) reported similar gradients for the western tropical Atlantic based on box core sediment assemblages ($\Delta\delta^{18}O_{men\text{-}sac} = 0.62‰$; $\Delta\delta^{18}O_{tum\text{-}sac} = 0.85‰$; these numbers are based on the average of all size fractions measured for each taxon). Complementing these isotope gradient data are foraminiferal census data demonstrating the dominance of mixed layer taxa over thermocline taxa in both the western equatorial Pacific and western tropical Atlantic (Ravelo and Fairbanks, 1992; Ravelo and Shackleton, 1995; this study). For example, the box core near Site 806 is dominated by mixed layer taxa *Globigerinita glutinata* (37%) and *Globigerinoides* spp. (32%), while thermocline taxa (*Pulleniatina obliqueloculata*, *Globigerinella aequilateralis*, *Neogloboquadrina dutertrei*, and *Globorotalia* spp.) collectively constitute <20% of the sediment assemblage (Table 2). A similar assemblage dominated by *Globigerinita* and *Globigerinoides* was recorded by nearby sediment trap studies (Yamasaki et al., 2008). Thus, a historical manifestation of the ancient WPWP (or proto-warm pool) should be relatively narrow oxygen isotopic gradients between thermocline and mixed layer taxa, and the dominance of mixed layer taxa in the planktic foraminiferal assemblages.

In the absence of a warm pool, isotopic gradients between mixed layer and thermocline taxa, as well as planktic foraminiferal census data, yield very different results (Fig. 3). For example, Ravelo and Fairbanks (1992) reported much greater oxygen isotope gradients between mixed layer and thermocline taxa from an eastern tropical Atlantic box core where the mixed layer is thinner and the thermocline is much shallower ($\Delta\delta^{18}O_{men\text{-}sac} = 1.23‰$; $\Delta\delta^{18}O_{tum\text{-}sac} = 2.09‰$). Similarly strong oxygen isotopic gradients characterize the EEP (e.g., Curry et al., 1983; Farrell et al., 1995a; Ravelo and Shackleton, 1995). In contrast to warm pool conditions, thermocline taxa, rather than mixed layer taxa, dominate the time-averaged sediment

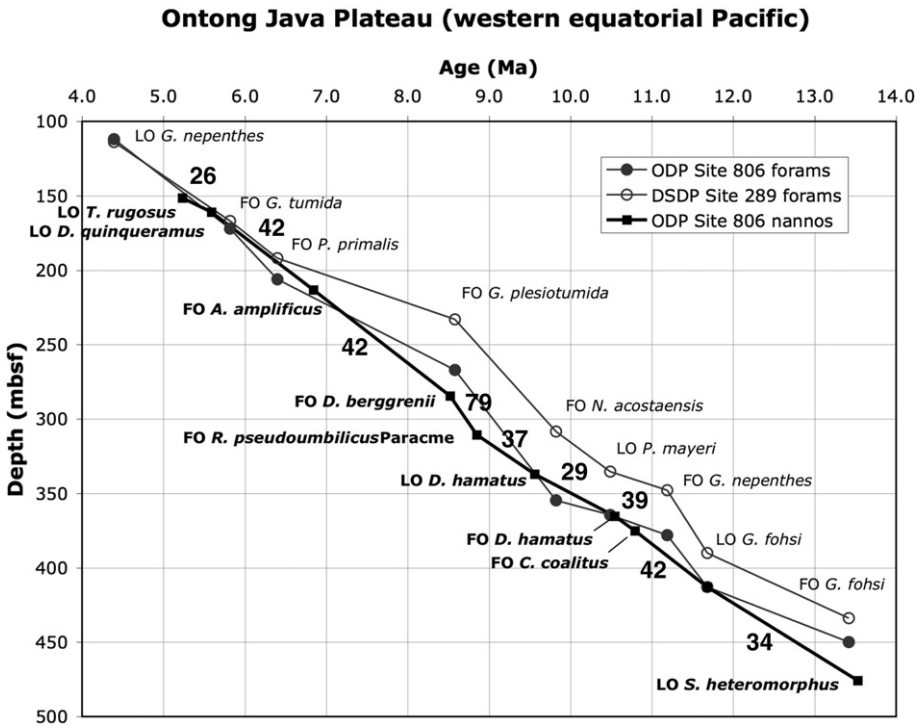

Fig. 2. Age–depth plot of planktic foraminifer (Chaisson and Leckie, 1993) and calcareous nannofossil (Takayama, 1993) datums at ODP Site 806, and comparison with planktic foraminifer datums (Srinivasan and Kennett, 1981; Hodell and Vayavananda, 1993) from nearby DSDP Site 289, Ontong Java Plateau, western equatorial Pacific. FO = first occurrence, LO = last occurrence. Planktic foraminifer datums in plain text, calcareous nannofossil datums in bold. Datum ages provided in the original publications have been updated to orbitally-tuned age models. Refer to Table 1 for details. The age model used in this paper is based on the calcareous nannofossil datums presented here. Numbers represent sediment accumulation rates (m/Myr) for line segments defined by calcareous nannofossil datums.

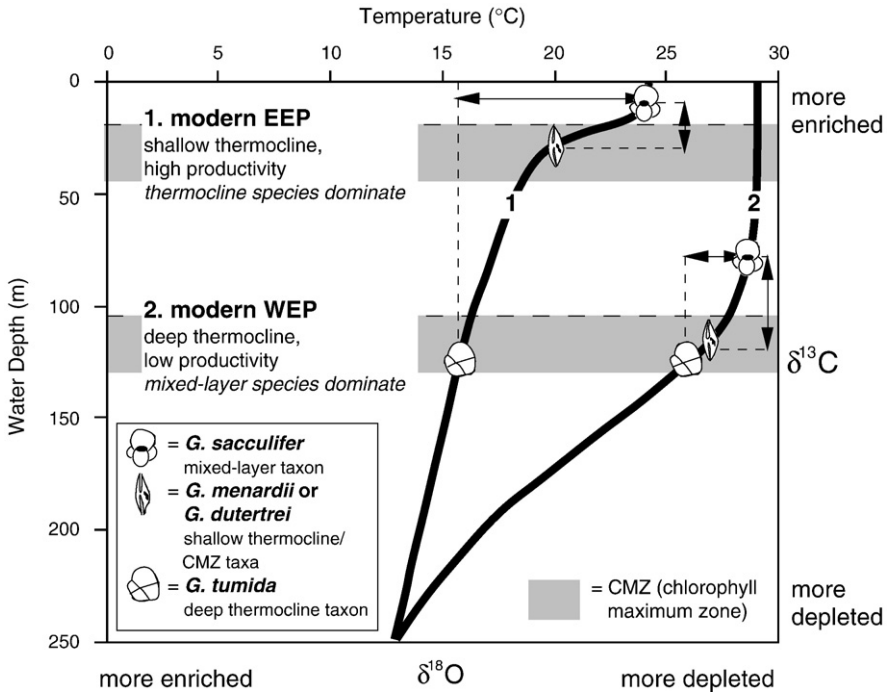

Fig. 3. Schematic representation of thermocline structure and stable isotopic gradients between mixed layer (*Globigerinoides sacculifer*), upper thermocline (*Neogloboquadrina dutertrei*, *Globorotalia menardii*), and deeper thermocline taxa (*Globorotalia tumida*, *Globoquadrina venezuelana*). See discussion in text. Modern WEP (line 2) and EEP (line 1) thermocline profiles averaged from 2°N to 2°S, at 160°E and 100°W, respectively, based on Levitus and Boyer (1994; as summarized in Patrick and Thunell, 1997). Under conditions of strong upwelling and shoaling of the thermocline as represented by the modern EEP (thermocline 1), the $\delta^{18}O$ gradient is enhanced between mixed layer and deeper thermocline taxa (vertical dashed lines and horizontal double-headed arrow), while the $\delta^{13}C$ gradient is reduced between mixed layer and upper thermocline taxa (horizontal dashed lines and vertical double-headed arrow). By contrast, the thick mixed layer and depressed thermocline in the modern WEP yields weaker $\delta^{18}O$ gradients between mixed layer and deeper thermocline taxa, and stronger $\delta^{13}C$ gradients between mixed layer and upper thermocline taxa.

assemblages in tropical regions characterized by seasonal upwelling and high biological productivity such as the eastern equatorial Pacific and Atlantic (e.g., Thunell et al., 1983; Thunell and Reynolds, 1984; Ravelo and Fairbanks, 1992; Chaisson, 1995; Ravelo and Shackleton, 1995; Chaisson and Ravelo, 1997; Patrick and Thunell, 1997; Chaisson and Ravelo, 2000).

For this study, we used *Globoquadrina venezuelana* as our deep thermocline taxon because *Globorotalia tumida*, or its ancestors, were not present through the entire upper middle Miocene and upper Miocene interval. We interpret small $\Delta\delta^{18}O_{ven\text{-}sac}$ gradients (analogous to the modern $\Delta\delta^{18}O_{tum\text{-}sac}$ values of Ravelo and Shackleton, 1995; Cannariato and Ravelo, 1997) as times when the mixed layer

Table 2
Population analysis and stable isotope analysis of multi-species, multi-size fraction planktic foraminifers, and a single benthic foraminifer *Planulina wuellerstorfi*, from a Ontong Java Plateau box core (sample MW 2.5-BC-37) located near ODP Site 806.

Site 806 0 Ma time slice (Sample MW 2.5-BC-37)						
Taxon	Percent abundance	# of size fractions	Avg. $\delta^{13}C$	$\delta^{13}C$ std. deviation	Avg. $\delta^{18}O$	$\delta^{18}O$ std. deviation
Globigerinoides rubber	23.9	4	1.098	0.723	−2.435	0.175
Globigerinita glutinata	37.1	5	0.021	0.813	−2.344	0.198
Globigerina bulloides	5.1	2	1.511	0.059	−2.342	0.004
Globoturborotalita rubescens	<0.3	1	−0.216	n/a	−2.187	n/a
Globigerinoides sacculifer	8.1	7	1.968	0.654	−2.118	0.186
Globigerinella aequilateralis	5.4	4	1.808	0.698	−1.966	0.328
Turborotalita humilis	n/a	2	1.727	0.696	−1.929	0.339
Globigerinoides conglobatus	<0.3	5	1.599	0.682	−1.677	1.048
Pulleniatina obliquiloqulata	10.2	3	1.161	0.194	−1.646	0.122
Orbulina universa	<0.3	1	2.119	n/a	−1.590	n/a
Globorotalia menardii	0.3	2	1.870	0.754	−1.461	0.028
Globorotalia ungulata	<0.3	1	1.336	n/a	−1.403	n/a
Globoquadrina conglomerata	<0.3	2	0.893	0.036	−1.384	0.061
Neogloboquadrina dutertrei	1.3	3	1.006	0.992	−1.301	0.356
Sphaeroidinella dehiscens	<0.3	2	1.685	0.313	−1.277	0.223
Globorotalia tumida	<0.3	1	1.773	n/a	−0.977	n/a
Globorotalia scitula	0.3	1	0.527	n/a	1.628	n/a
Planulina wuellerstorfi	0.5	1	0.299	n/a	2.518	n/a

Percent abundance refers to taxon relative abundance. Percent abundance values of <0.3% refers to zero counts of that taxon in the population analysis, though enough tests were collected from the processed sample for isotope analyses. Number of size fractions refers to the number of analyses for each individual species. $\delta^{13}C$ and $\delta^{18}O$ are the averages for all size fraction analyzed. $\delta^{13}C$ and $\delta^{18}O$ Std. Deviation are the standard deviations of the carbon and oxygen isotope values obtained for all size fractions analyzed. Taxa having small standard deviations had tests that varied little during ontogeny (growth), while those taxa having high standard deviations changed significantly during ontogeny. Standard deviation values of taxa having only one size fraction analyzed are assigned n/a (not applicable). Taxa are arranged by increasing average $\delta^{18}O$ values (i.e., lowest to highest).

was thick and the thermocline depressed, while much higher $\Delta\delta^{18}O_{ven\text{-}sac}$ gradients represent times when the thermocline shoaled and there was a much greater temperature contrast between the water mass habitats of the mixed layer and thermocline planktic foraminifers (Fig. 3). *Neogloboquadrina dutertrei* was not present through the study interval so we used *G. menardii* as our upper thermocline taxon. We interpret the stratigraphic changes in $\delta^{18}O$ of *G. menardii* to reflect its preference for the chlorophyll maximum zone in the upper water column (Ravelo and Fairbanks, 1992), analogous to the behavior of *N. dutertrei*/*N. humerosa* in the Pliocene of the equatorial Pacific (Cannariato and Ravelo, 1997) (Fig. 3).

Productivity can be gauged by relative changes in the carbon isotopes of the mixed layer taxon (ML; $\delta^{13}C_{ML}$) and the carbon isotope gradient between mixed layer and thermocline taxa (UTH, DTH; $\Delta\delta^{13}C_{ML\text{-}UTH}$, $\Delta\delta^{13}C_{ML\text{-}DTH}$). Ravelo and Fairbanks (1995) studied the $\delta^{13}C$ of multiple size fractions of fifteen different species from three box core tops representing end-member hydrographic conditions spanning the tropical Atlantic. A comparison of the western site with the eastern site reveals a greater $\delta^{13}C$ gradient between *Globorotalia menardii* and *G. sacculifer* in the western warm pool site (~1.2‰) compared with the eastern site (~0.5‰). Likewise, the $\delta^{13}C$ gradient is greater between *G. tumida* and *G. sacculifer* in the western warm pool site (~1.4‰) compared with the eastern site (~0.6‰).

In summary, oxygen and carbon isotope gradients between mixed layer and thermocline taxa, in combination with population analyses, are reliable proxies for changes in the structure of the upper water column, specifically, the position of the thermocline relative to the photic zone and thickness of the mixed layer. Tropical thermocline taxa are a significant component of the sediment assemblages when productivity is moderate to high as a result of a thinner mixed layer and shoaling of the thermocline by upwelling of nutrient-rich water. This creates a larger $\delta^{18}O$ gradient between the deep thermocline and mixed layer taxa, but a reduced $\delta^{13}C$ gradient between the upper thermocline and mixed layer taxa (Fig. 3). Conversely, mixed layer taxa dominate the assemblages when productivity is low as a result of a thicker mixed layer and deeper thermocline as in the situation characterized by warm pool conditions. Under these latter conditions, the $\delta^{18}O$ gradient between the thermocline and mixed layer taxa is reduced, while the $\delta^{13}C$ gradient may be expanded (Fig. 3).

4. Time series results

4.1. Oxygen isotopes

At Site 806, a positive excursion in the oxygen isotope ratio of benthic foraminifera ($\delta^{18}O_B$) at the base of the record (~13.2–13.0 Ma) likely coincides with the Mi4 event that marks a major pulse of ice-sheet growth in Antarctica (Miller et al., 1991; Wright et al., 1991, 1992; Flower and Kennett, 1993, 1994; Westerhold et al., 2005). After this excursion, the $\delta^{18}O_B$ record increases by >0.5‰ for the remainder of the study interval with several positive excursions that correlate with Mi5 (~11.7–11.5 Ma), Mi6 (~10.6–10.4 Ma), and possibly Mi7 (~9.3–9.2 Ma); as well as other positive excursions at ~7.7–7.6, 7.4–7.3, 7.0–6.9, and 5.9–5.8 Ma (Fig. 4A). A number of these latter events correlate with the ODP Site 999 record from the deep Caribbean (Bickert et al., 2004).

Among the three planktic species in the time series, there are two repeating trends in the relationship of one species with another. First, in two intervals (13.6–11.6 Ma, 8.6–6.5 Ma), the deeper thermocline species ($\delta^{18}O_{DTH}$: *Globoquadrina venezuelana*) has significantly higher $\delta^{18}O$ values than both the upper thermocline species ($\delta^{18}O_{UTH}$: *G. menardii*) and mixed layer species ($\delta^{18}O_{ML}$: *G. sacculifer*). This results in an expanded isotopic gradient between the deeper thermocline and mixed layer (large $\Delta\delta^{18}O_{DTH\text{-}ML}$), and a reduced gradient between the upper thermocline and mixed layer (small $\Delta\delta^{18}O_{UTH\text{-}ML}$; Fig. 4B). Second, in the intervals that follow this trend (11.6–9.6 Ma, 6.5–6.0 Ma), the gradient between the deeper thermocline species and mixed layer species is greatly reduced (much smaller $\Delta\delta^{18}O_{DTH\text{-}ML}$), but the upper thermocline species becomes distinctly more positive relative to the mixed layer species with isotopic values much closer to the deep thermocline species (larger $\Delta\delta^{18}O_{UTH\text{-}ML}$ and small $\Delta\delta^{18}O_{DTH\text{-}UTH}$).

The first trend (intervals 1 and 4 in Fig. 4A) is interpreted as a shallow thermocline and thin mixed layer, while the second trend (intervals 2 and 5 in Fig. 4A) is interpreted as a deep thermocline and thick mixed layer following the modern analog of *G. sacculifer*–*G. tumida* gradients in different tropical hydrographies (e.g., Ravelo and Fairbanks, 1992; Ravelo and Shackleton, 1995). The transition from trend 1 to trend 2 is accompanied by decreasing deep thermocline values that precede decreasing mixed layer values, suggesting that the deep thermocline waters warmed prior to surface waters. The 9.6–8.6 Ma interval separating the two repeated trends is characterized by reduced but highly variable gradients between the mixed layer, upper thermocline, and deeper thermocline taxa.

The gradient between *Globoquadrina venezuelana* and *G. sacculifer* ($\Delta\delta^{18}O_{DTH\text{-}ML}$) changes in step-like fashion, which we use to define five intervals through the studied section (Fig. 4A and B). These steps reflect significant changes in the structure of the upper water column and they parallel changes observed in the planktic foraminifer assemblages (discussed below). The high variability of *G. venezuelana* observed in some intervals is likely to reflect a primary signal and not diagenesis because species of *G. fohsi*, *G. menardii*, and *G. sacculifer* do not display such inter-sample isotopic variability. Similar high variability in middle Miocene age *G. venezuelana* was observed in the western equatorial Pacific by Gasperi and Kennett (1993a,b) and Norris et al. (1993), and in the central equatorial Pacific by Vincent and Killingley (1985). Gasperi and Kennett (1993b, p. 242) concluded that the variability of *G. venezuelana* through the middle and late Miocene of nearby DSDP Site 289 reflected its "greater sensitivity to changes in the vertical thermal structure."

Prior to the evolution of *Globorotalia* (*Menardella*) *menardii*, we used a continuous record of *Globorotalia (Fohsella) fohsi* as a proxy of the upper thermocline layer because *G. praemenardii* was discontinuous and rare at Site 806 (Fig. 4A and B). A single sample at ~12.4 Ma containing *G. praemenardii* rather than *G. fohsi*, yields similar oxygen and carbon stable isotopic values as *G. fohsi* in adjacent samples. After ~12.4 Ma, *G. fohsi* (and *G. praemenardii*) gradually diverge from *G. sacculifer* $\delta^{18}O$ values as described by Hodell and Vayavananda (1993) and Norris et al. (1993), but the gradient between the upper thermocline and mixed layer taxa is <0.5‰. It is likely that our smaller measured gradient between *G. fohsi* and *G. sacculifer* is a consequence of the discrete size fraction (355–425 μm) we used, whereas Hodell and Vayavananda (1993) and Norris et al. (1993) used larger and isotopically more positive specimens as the *G. fohsi* lineage became larger and fully keeled after 13 Ma. For example, the Hodell and Vayavananda (1993) study shows increased *G. fohsi* $\delta^{18}O$ values in parallel with increased specimen size.

Our time series data from ODP Site 806 show that the benthic and mixed layer records do not track each other. This observation suggests that there have been changes in surface water temperatures and/or salinity in the WEP, particularly after ~11.6 Ma when the two records gradually diverge. The late Miocene mixed layer $\delta^{18}O_{sac}$ values are ~0.5–1.5‰ more positive than Holocene values (−1.92‰, *G. sacculifer* 250–300 μm size fraction; from box core near Site 806; Table 2). One explanation is that surface waters in the vicinity of Site 806 were saltier prior to the emergence of Halmahera Island and the equator crossing of New Guinea in the last 5 Myr (Cane and Molnar, 2001; Molnar and Cane, 2002). With no Halmahera Island, and with New Guinea still south of the equator, Indonesian Throughflow would be supplied primarily by saltier South Pacific waters compared to the fresher North Pacific waters that feed the ITF today (Fig. 1; Morey et al., 1999; Rodgers et al., 2000). Less precipitation in the WEP prior to strengthening of the East Asian monsoon (e.g., Rea, 1992; Filippelli, 1997; Wan et al., 2006) may also account for the higher $\delta^{18}O_{sac}$ values during the Miocene. A third possible explanation is that middle to late Miocene sea surface temperatures were

cooler in the WEP. Preliminary Mg/Ca paleotemperature estimates based on *G. sacculifer* from three time slices at Site 806 (6.2, 7.5, and 8.9 Ma; 4 to 5 samples each with replicate analyses) yield average values slightly cooler than present (27.3 °C, 28.4 °C, and 28.2 °C, respectively; Dekens et al., 2002 paleotemperature equation; T. Quinn, 2006, personal communication; Table 3). Taken together, late Miocene surface waters of the WEP were likely somewhat saltier and slightly cooler than present conditions accounting for the higher $\delta^{18}O_{sac}$ values relative to modern *G. sacculifer* from the 250–300 μm size fraction.

4.2. Carbon isotopes

The high benthic $\delta^{13}C$ values observed at ~13.2 Ma correspond with the final carbon burial event (CM6) of the middle Miocene Monterey Carbon Excursion (Vincent and Berger, 1985; Flower and Kennett, 1994). Benthic $\delta^{13}C$ values at Site 806 rapidly decrease by 1‰ after 8.0 Ma but then decline less rapidly after 6.8 Ma corresponding with the "Chron 6 Carbon Shift" of Vincent et al. (1980) (Fig. 4C). This late Miocene negative $\delta^{13}C$ shift has been attributed to 1) increased production and burial of biogenic sediments (Vincent et al., 1980), 2) increased carbonate dissolution in the deep-sea (e.g., Berger and Vincent, 1981; Diester-Haass et al., 2005), 3) increased erosion of organic-rich terrigenous and shallow marine sediments associated with Antarctic glaciation and sea level fall (Berger and Vincent, 1981; Bickert et al., 2004), and/or 4) shift from C_3 to C_4-dominated terrestrial floras (Cerling et al., 1997). The ~8.0–6.8 Ma interval also correlates with an interval of increased deep-sea hiatus frequency (Keller and Barron, 1983; Spencer-Cervato, 1998) and increased production of Northern Component Water (Lear et al., 2003).

Globoquadrina venezuelana ($\delta^{13}C_{DTH}$) carbon isotope values display benthic-like values and high inter-sample variability in the early part of the record (Fig. 4C). By ~11.6 Ma, *G. venezuelana* $\delta^{13}C$ values rapidly converge with *Globorotalia menardii* ($\delta^{13}C_{UTH}$), and then track *G. menardii* values until ~6.0 Ma. Planktic $\delta^{13}C$ values converge at ~9.0–8.8 Ma, coincident with the near collapse of the widespread calcareous nannofossil genus *Reticulofenestra* at Site 806 (Takayama, 1993)

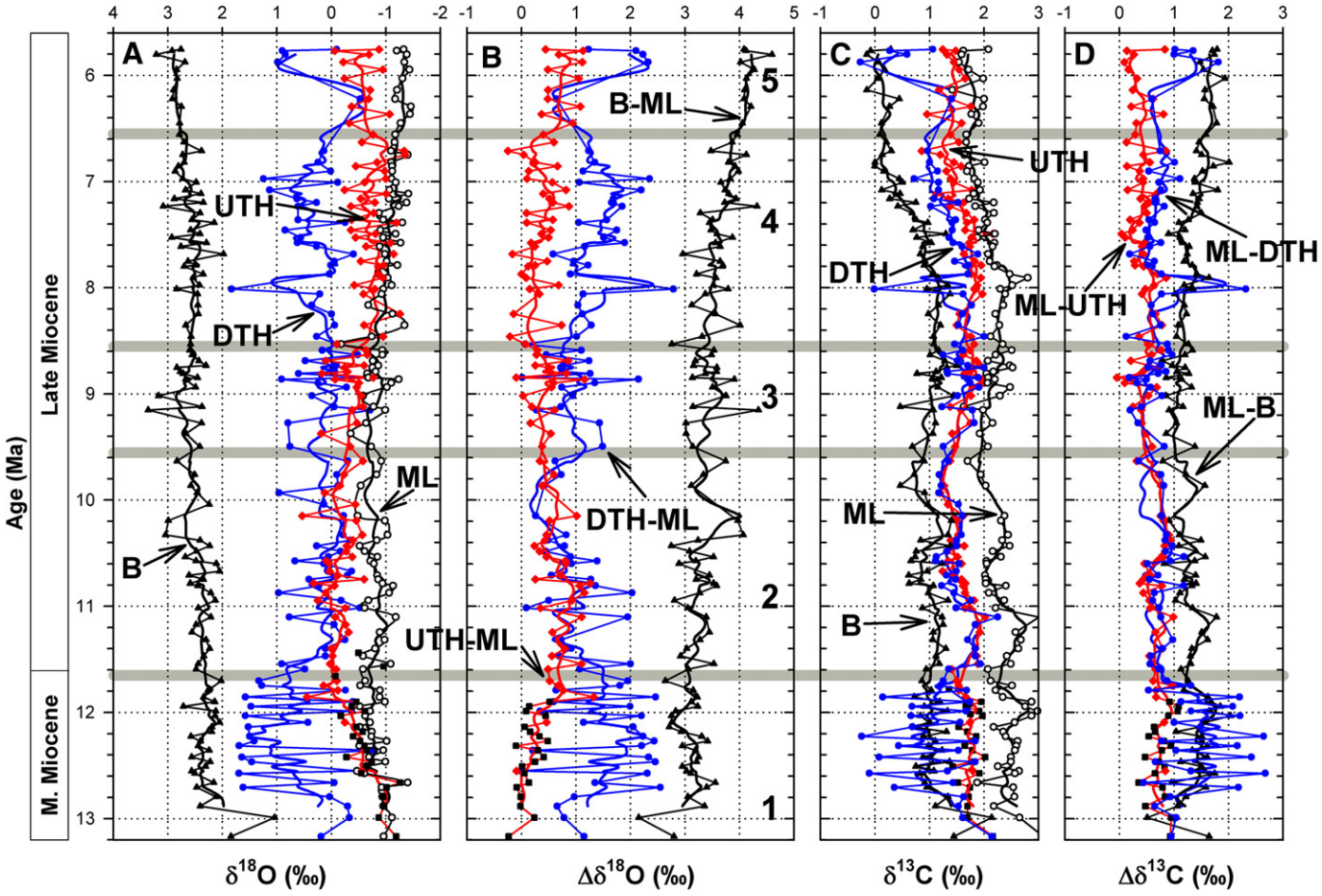

Fig. 4. Continuous planktic foraminiferal stable isotope and population assemblage data for ODP Site 806. Panel A) continuous record of benthic (B; black triangles), deep thermocline (DTH; blue circles = *G. venezuelana*), upper thermocline (UTH; red diamonds = *G. menardii*, black squares = *G. fohsi*) and mixed layer (ML; open circles = *G. sacculifer*) stable oxygen isotope ratios ($\delta^{18}O$). Panel B) oxygen isotope gradient between mixed layer and upper thermocline species ($\Delta\delta^{18}O_{UTH\text{-}ML}$; red diamonds and black squares), between mixed layer and deep thermocline species ($\Delta\delta^{18}O_{DTH\text{-}ML}$; blue circles), and between mixed layer and benthic species ($\Delta\delta^{18}O_{B\text{-}ML}$; black triangles). Panel C) continuous record of benthic (black triangles), deep thermocline (blue circles), upper thermocline (red diamonds and black squares) and mixed layer (open circles) stable carbon isotopes ($\delta^{13}C$). Panel D) carbon isotope gradient between mixed layer and upper thermocline species ($\Delta\delta^{13}C_{ML\text{-}UTH}$; red diamonds and black squares), between mixed layer and deep thermocline species ($\Delta\delta^{13}C_{ML\text{-}DTH}$; blue circles), and between mixed layer and benthic species ($\Delta\delta^{13}C_{ML\text{-}B}$; black triangles). Panels A–D depict five point running averages, bold numbers 1–5 refer to the interval numbers described in the text. Panel E) percent thermocline species abundances (Thermocline assemblage 1 (dark blue) = *Neogloboquadrina* spp., *Globorotalia* spp.; Thermocline assemblage 2 (light blue) = *Globoquadrina dehiscens* and species of *Sphaeroidinellopsis*). Panel F) mixed layer assemblage 2 abundances (yellow; *Globoturborotalita* spp. — except *G. nepenthes*, *Dentoglobigerina altispira*, *Paragloborotalia* spp.), black curve is radiolarian abundances relative to total foraminifera. Panel G) mixed layer assemblage 1 abundances (*Globigerinoides* spp., *Globigerinita glutinata*), *Reticulofenestra* spp. (a calcareous nannofossil genus) counts represented by thick line with open circles (data from Takayama, 1993). Panel H) Other species (i.e., planktic species not included in panels E, F, G; black curve), percent foraminiferal fragments (green curve), Atlantic–Pacific carbon gradient ($\Delta\delta^{13}C_{A\text{-}P}$; thick line, redrawn from Lear et al. (2003)). Panels E–H also depict five point running averages, bold numbers 1–5 refer to the interval numbers described in the text, Mi4 through Mi6 refer to Miocene oxygen isotope excursions (Wright et al., 1992; Miller et al., 1998). (For interpretation of the references to color in this figure legend, the reader is referred to the web version of this article.)

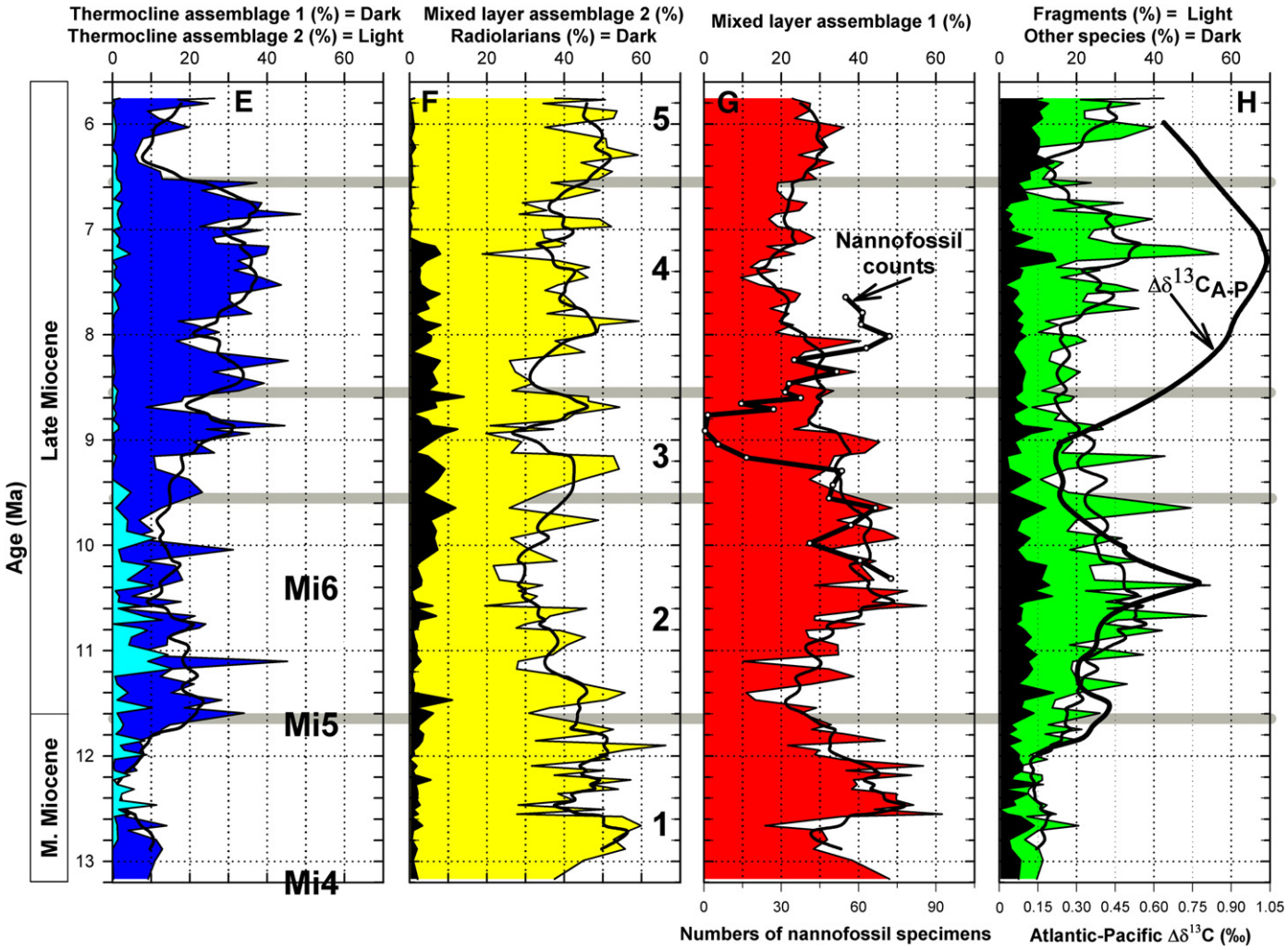

Fig. 4 (*continued*).

indicating minimal upper water column $\delta^{13}C$ gradients ($\Delta\delta^{13}C_{ML\text{-}UTH}$, $\Delta\delta^{13}C_{ML\text{-}DTH}$) (Fig. 4D). Also noteworthy in the Site 806 record are the minimal upper water column $\delta^{13}C$ gradients at ~7.8–7.4 Ma. At 6 Ma, *G. venezuelana* $\delta^{13}C$ diverges from *G. menardii*, taking on benthic-like values once again.

4.3. Foraminiferal test fragments

Foraminiferal test fragments (a proxy for dissolution) at Site 806 were at a minimum from 13.2 to 12.0 Ma (Fig. 4H). After 12 Ma, test fragmentation increased gradually, reaching a peak between ~11 and 10 Ma. This pattern of increasing test fragmentation generally parallels the increase in benthic foraminiferal carbon isotopic gradient between the deep Pacific and the Atlantic ($\Delta\delta^{13}C_{A\text{-}P}$) (Lear et al., 2003), which is a proxy for Northern Component Water production in the northern North Atlantic. Fragments decline markedly from ~9.6–8.8 Ma and then remain low until ~7.8 Ma. Foraminiferal fragments increased after 7.8 Ma, once again in parallel with the $\Delta\delta^{13}C_{A\text{-}P}$ gradient (Lear et al., 2003) (Fig. 4H). After peaking at ~7.2 Ma, test fragments and other dissolution proxies sharply declined, reaching a low at ~6.6–6.2 Ma. Test fragmentation increases after 6.2 Ma. Abundances of the thick-walled genus *Sphaeroidinellopsis* increase slightly in the intervals of increased test fragmentation (Fig. 5), but the relative abundances of porous, thinner-walled taxa such as *Globigerinoides* do not track fragmentation trends suggesting that dissolution has not greatly affected the planktic foraminiferal assemblages.

5. Assemblage results

Stratigraphic changes in planktic foraminiferal assemblages closely track changes in the stable isotopes. These natural groupings are also supported by multivariate statistical techniques, including R-mode (species associations) Principal Components Analysis and Q-mode (sample groupings) Cluster Analysis, but are not discussed here because of space limitations. Mixed layer taxa (assemblages 1 and 2; Fig. 4F and G) greatly dominate the record from 13.2 to ~11.7 Ma. A significant change in assemblage composition at ~11.7 Ma is caused primarily by the sharp decline in the mixed layer taxon *Globigerinoides*. Thermocline species abundances increase in the interval from 11.7 to 10.0 Ma, but they are generally <20% of the assemblages prior to ~9.0 Ma (Fig. 4E). Thermocline species begin to increase in relative abundance after the appearance of the *Neogloboquadrina acostaensis–N. humerosa–N. dutertrei* lineage at ~9.8 Ma. Their abundances are generally >30% from ~9.0 to ~6.5 Ma, then sharply decline at 6.5 Ma before increasing again at ~6.1 Ma (Fig. 4E). The rapid drop in relative abundances of *Neogloboquadrina* spp. and *Globorotalia* spp. at ~6.5 Ma coincides with the appearance of *Pulleniatina primalis*, a characteristic thermocline genus of the western equatorial Pacific today (Fig. 5).

Trends in planktic foraminiferal simple diversity generally track thermocline species abundance, particularly after ~9 Ma when both

Table 3
Preliminary study of (near-)sea surface temperatures based on Mg/Ca ratios of Site 806 mixed layer-dwelling planktic foraminifer *Globigerinoides sacculifer* from three time slices (~6.2, 7.5, and 8.9 Ma).

Hole	Core-section, interval (cm)	Replicate	Ca conc. (ppm)	Mg/Ca (mmol/mol)	Dekens et al. (2002) Eq 6	Sr/Ca (mmol/mol)
806B	34H-1, 59	R1	15.6	3.714	28.47	1.162
806B	34H-1, 59	R2	7.0	3.676	28.35	1.143
806B	34H-1, 144	R1	1.9	4.955	31.67	1.101
806B	34H-1, 144	R2	5.3	4.306	30.11	1.141
806B	34H-2, 79	R1	5.7	3.440	27.62	1.190
806B	34H-2, 79	R2	12.7	3.413	27.53	1.196
806B	34H-3w, 13	R1	6.3	3.360	27.36	1.161
806B	34H-3w, 13	R2	10.1	3.752	28.58	1.156
806B	34H-4, 32	R1	3.0	3.894	28.99	1.148
806B	34H-4, 32	R2	2.4	3.379	27.42	1.125
806B	26H-4, 70	R1	11.2	3.656	28.29	1.162
806B	26H-4, 70	R2	10.2	3.550	27.96	1.154
806B	26H-4, 104	R1	17.4	3.742	28.55	1.154
806B	26H-4, 104	R2	20.9	3.631	28.22	1.151
806B	26H-5, 12	R1	9.6	3.619	28.18	1.135
806B	26H-5, 12	R2	6.8	3.727	28.51	1.137
806B	26H-5, 111	R1	33.2	3.863	28.90	1.142
806B	26H-5, 111	R2	18.0	3.911	29.04	1.143
806B	26H-6, 35	R1	14.2	3.749	28.57	1.158
806B	26H-6, 35	R2	13.4	3.579	28.05	1.163
806B	21H-1, 111	R1	25.4	2.978	26.01	1.179
806B	21H-1, 111	R2	21.1	2.951	25.91	1.176
806B	21H-2, 54	R1	19.3	3.389	27.45	1.170
806B	21H-2, 54	R2	14.4	3.274	27.07	1.158
806B	21H-2, 100	R1	24.4	3.611	28.15	1.176
806B	21H-2, 100	R2	24.5	3.719	28.48	1.168
806B	21H-2, 147	R1	31.9	3.347	27.31	1.178
806B	21H-2, 147	R2	17.8	3.508	27.83	1.180

diversity and thermocline species abundance increase significantly (Fig. 6). A sharp drop in planktic foraminiferal simple diversity coincides with the rapid decline in thermocline species at ~6.5 Ma.

Radiolarians increase in abundance at ~10.1 Ma and remain >5% of the >150 μm size fraction until ~7.2 Ma, roughly coincident with elevated abundances of the planktic foraminiferal genus *Neogloboquadrina* (Fig. 4F). The elevated abundances of radiolarians and *Neogloboquadrina* spp. are indicative of relatively higher productivity.

Abundances of thermocline species and mixed layer assemblage 2 display high amplitude variability from 9.6 Ma to 8.6 Ma. This is an interval that also shows dramatic changes in the calcareous nannofossil assemblages (Takayama, 1993). Noteworthy is the sharp increase in relative abundance of *Globoturborotalita nepenthes* and *Neogloboquadrina* spp. ~9.0–8.8 Ma (coincident with the crash in the nannofossil genus *Reticulofenestra*), and then again ~7.6–7.4 Ma (Fig. 5). Both of these intervals correspond with minimal upper water column $\delta^{13}C$ gradients ($\Delta\delta^{13}C_{ML\text{-}TH}$, $\Delta\delta^{13}C_{ML\text{-}DTH}$) indicative of elevated productivity (Fig. 4D). The upper water column $\delta^{13}C$ gradient ($\Delta\delta^{13}C_{ML\text{-}TH}$) once again collapses after 6.1 Ma, which coincides with renewed abundances of *Neogloboquadrina* (Figs. 4D and 5).

In addition to the relationship between increased relative abundances of *Neogloboquadrina* and reduced upper water column $\delta^{13}C$ gradient, there also appears to be a relationship between trends in upper water column oxygen isotope values ($\delta^{18}O_{UTH}$) and relative abundances of *Neogloboquadrina* and *Globorotalia* (Fig. 7). For example, *Globorotalia* spp. show peaks in abundance ~11.6–11.0 Ma, ~10.6–10.0 Ma, ~8.6–8.2 Ma, and ~7.0–6.7 Ma. All four of these intervals correspond with times of decreasing $\delta^{18}O_{UTH}$ values relative to $\delta^{18}O_{ML}$ values suggesting warming of the upper thermocline. Conversely, *Neogloboquadrina* spp. display peaks in abundance ~9.2–8.7 Ma, 8.2–7.2 Ma, and after 6.1 Ma. These intervals correspond with increasing $\delta^{18}O_{UTH}$ values relative to $\delta^{18}O_{ML}$ values suggesting cooling of the upper thermocline (Fig. 7).

Neither the relative abundances of the individual taxa (Fig. 5), nor the four different assemblage groups (Fig. 4E–G) closely track the foraminiferal fragment values (Fig. 4H) indicating that assemblage data are not significantly biased by dissolution.

6. Discussion

6.1. Paleoceanography of the Western Equatorial Pacific through the late Miocene

The discussion that follows is divided into five intervals based on changes in the isotopic and biotic character of Site 806 (Figs. 4–7).

6.2. Pre-closure trans-Equatorial circulation (Interval 1: 13.2–11.6 Ma)

Interval 1 is dominated by mixed layer species, particularly species of the genus *Globigerinoides* (Fig. 5). During early middle Miocene time, mixed layer species dominated the equatorial Pacific, although there was a west–east asymmetry in mixed layer species distribution with *Globigerinoides* dominating the assemblages in the WEP and *Paragloborotalia mayeri/siakensis* dominating in the EEP (Keller, 1985; Kennett et al., 1985). The dominance of mixed layer taxa and paucity of thermocline species at ODP Site 806 suggests a relatively deep thermocline (Fig. 4E–G; Keller, 1985; Kennett et al., 1985; Chaisson and Leckie, 1993; Hodell and Vayavananda, 1993). However, the highly variable oxygen and carbon isotope values of *G. venezuelana* (Fig. 4A and C) suggest that the deeper thermocline was very dynamic in the WEP during the middle Miocene when the Indonesian and Central American Seaways were still open to intermediate waters (Keller, 1985; Kennett et al., 1985; Duque-Caro, 1990; Droxler et al., 1998), and perhaps deep waters from the North Atlantic (Nisancioglu et al., 2003).

The measured high inter-sample variability in the *Globoquadrina venezuelana* record is extreme compared with *Globorotalia fohsi* s.l., *G. praemenardii*, and *Globigerinoides sacculifer*. We interpret the large fluctuations in *G. venezuelana* oxygen and carbon isotope values as due to general instability in the structure or depth of the deep WEP thermocline at this time. For example, many of the pre-11.6 Ma values indicate that the thermocline was relatively shallow based on the large isotopic gradient between *G. venezuelana* and *G. sacculifer* ($\Delta\delta^{18}O_{DTH\text{-}ML}$; Fig. 4B). At other times the thermocline deepened as suggested by the reduced gradient values. Such isotopic variability indicates that a stable warm pool did not exist prior to 11.6 Ma. Perhaps instability in the upper water column above Site 806 was related to equator crossing during the pre-11.6 Ma interval and the dynamic nature of the equatorial divergence transition zone. The very low carbon isotope values of *G. venezuelana* are similar to benthic values suggesting perhaps the presence of an oxygen minimum zone (OMZ) in the WEP at this time (Fig. 4C). However, the absence of the planktic foraminifer genus *Streptochilus* (Chaisson and Leckie, 1993; Resig, 1993), a taxon attributable to high tropical productivity and OMZ development, together with the dominance of mixed layer planktic foraminifer species, do not support this latter interpretation.

Abundances of non-keeled *Globorotalia (Fosella) lenguaensis*, the last species of the *Fosella* lineage, significantly increase in the 12.0–11.6 Ma interval (Chaisson and Leckie, 1993; Fig. 5). This interval also coincides with the last occurrence of *G. fohsi* (~11.68 Ma) and the first occurrence of *G. menardii* (~11.65 Ma). Our isotope paleoecologic analyses indicate that *G. lenguaensis* was a thermocline species (Nathan, 2005). The evolutionary turnover of thermocline taxa and increased abundances of thermocline-dwelling species during the Interval 1–Interval 2 transition suggest a significant change in the upper water column structure (Fig. 6). Furthermore, the sharp decline in *G. venezuelana* oxygen isotope values and stabilization of carbon isotope values after ~12 Ma indicate warming of the deep thermocline (Fig. 7). We suggest that the development of stable stratification due

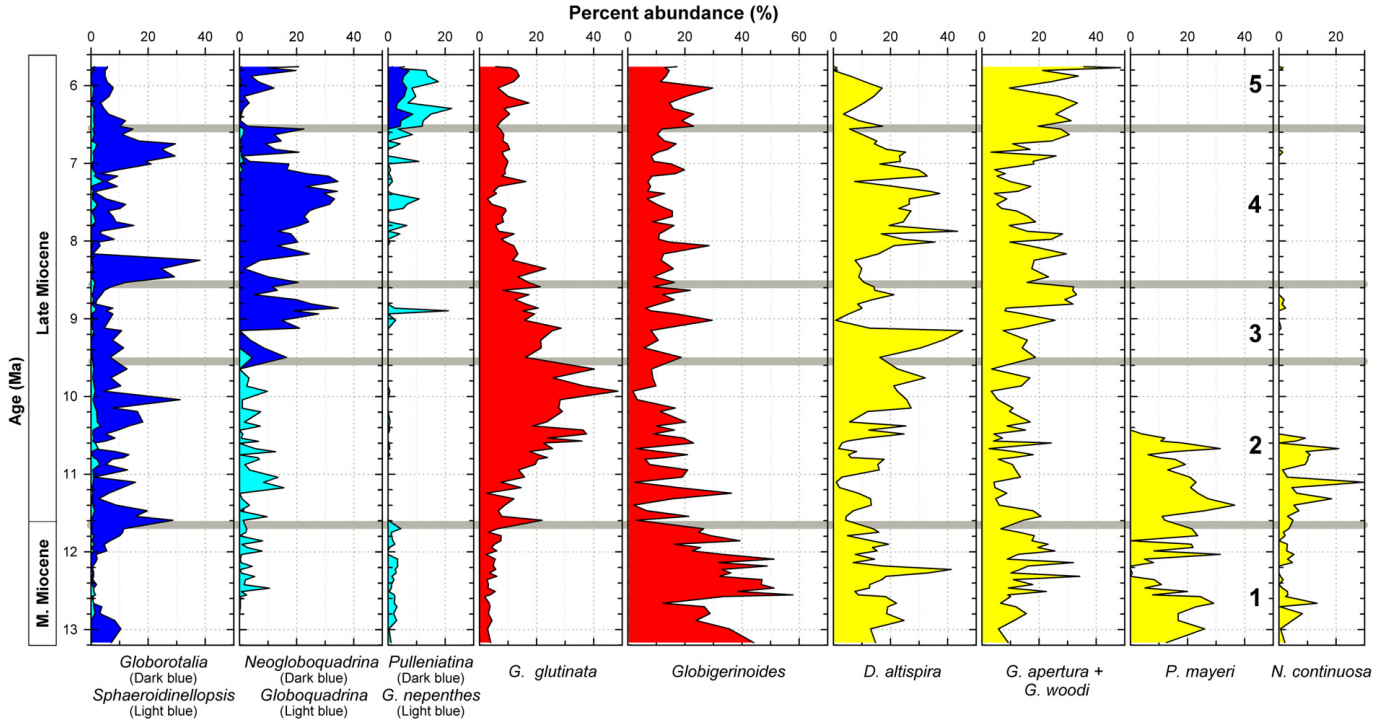

Fig. 5. Relative abundances of major taxa through Site 806 based on counts of at least 300 specimens. See text for explanation of the four groups.

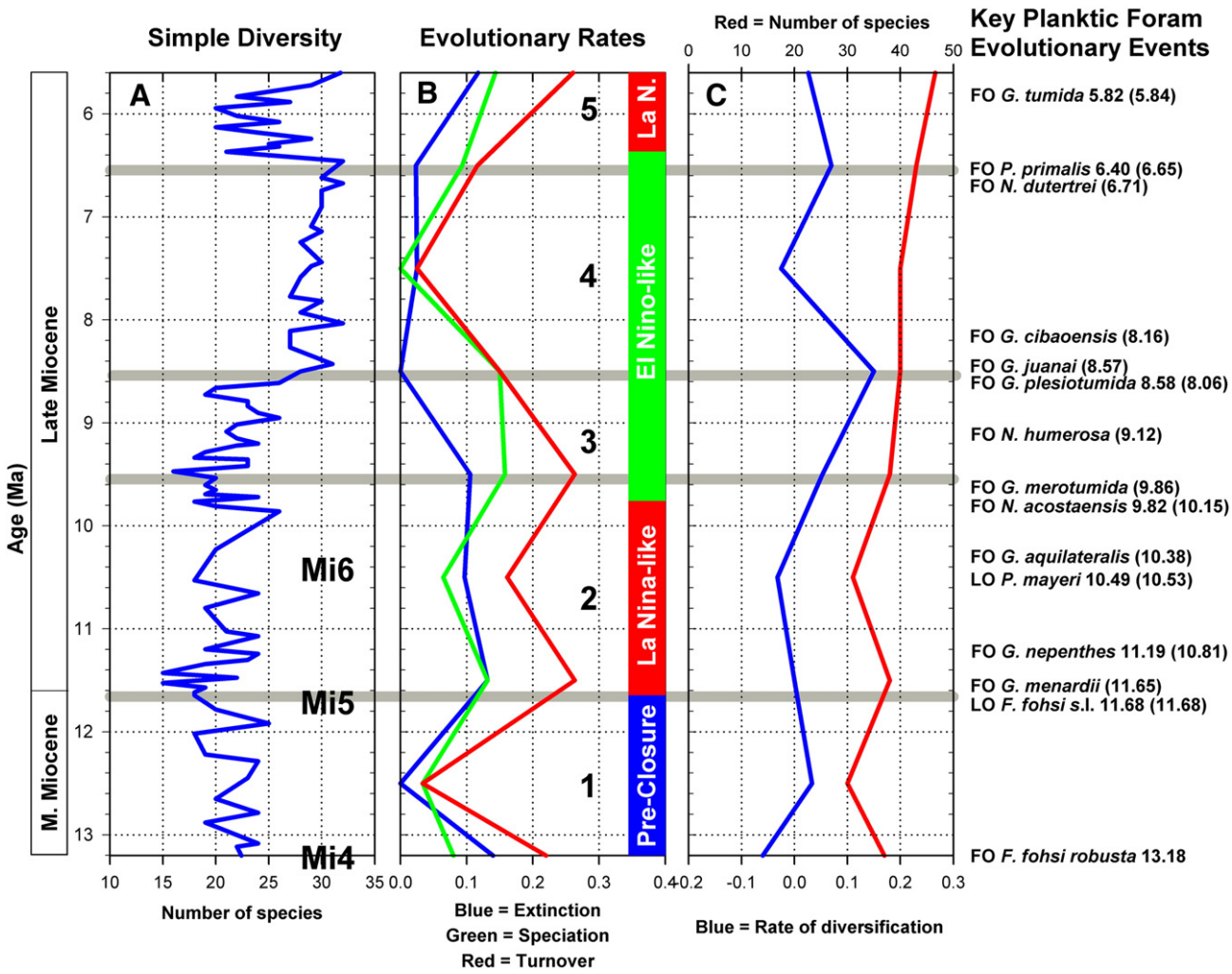

Fig. 6. Simple diversity of planktic foraminiferal species through the study interval of Site 806 (panel A) and calculated evolutionary rates (per million year rates; panels B and C) based on Chaisson and Leckie (1993) and updated to an age model based on orbitally-tuned datums of Chaisson and Pearson (1997; refer to Table 1). Key Planktic Foram Evolutionary Events highlight the evolutionary turnover of thermocline-dwelling planktic foraminifers in the middle to late Miocene transition at Site 806 (*P. mayeri* was a mixed layer taxon). Data from Chaisson and Leckie (1993) updated to orbitally-tuned datum levels of Chaisson and Pearson (1997).

to the formation of the proto-warm pool created stable conditions in the WEP and facilitated the evolutionary turnover of thermocline species ~11.7–11.6.

6.3. Two-step formation of a proto-warm pool (Interval 2: 11.6–9.6 Ma)

The Interval 1–Interval 2 transition marks a major change in the structure of the upper water column ~11.7–11.6 Ma as supported by the following evidence: 1) changes in the population structure of planktic foraminiferal assemblages at Site 806, particularly the mixed layer assemblages as seen by the sharp decline in *Globigerinoides* spp. and the rise of *Globigerinita glutinata* (Fig. 5); 2) the extinction of *Globorotalia (Fosella) fohsi* s.l. (*G. fohsi fohsi*, *G. fohsi lobata,* and *G. fohsi robusta*), the evolution of thermocline species (e.g., *G. menardii*, *Globoturborotalita nepenthes*, *Globigerinella aequilateralis*, *Neogloboquadrina acostaensis*, and *G. merotumida*), and the extinction of long-ranging mixed-layer taxa (e.g., *Paragloborotalia mayeri*, *Neogloboquadrina continuosa*, and *G. subquadratus*) (Chaisson and Leckie, 1993) (Fig. 6); 3) sharp decrease in oxygen isotope gradient between the deep thermocline and mixed layer taxa ($\Delta\delta^{18}O_{DTH\text{-}ML}$) beginning at ~11.8 Ma as *G. venezuelana* values converge with those of *G. menardii* (Fig. 7); 4) sharp decrease in mixed layer oxygen isotope values ($\delta^{18}O_{ML}$) at ~11.6–11.1 Ma and again at ~10.5–10.2 Ma (Fig. 7); 5) increase in the relative abundances of thermocline species (Fig. 5); and 6) increased percentages of foraminiferal test fragments at Site 806 in parallel with a sharp increase in the deep sea carbon gradient between the Atlantic and the Pacific ($\Delta\delta^{13}C_{A\text{-}P}$; Fig. 4H). The changing structure of the upper water column in the tropics, specifically the thickness of the mixed layer and the depth of the thermocline relative to the euphotic zone, may have been important physical and chemical stimuli of evolutionary activity noted above (Fig. 6).

There are two intervals with declining thermocline and mixed layer $\delta^{18}O$ values: ~11.8–11.2 Ma and ~10.8–10.2 Ma, which we interpret as times of thermocline warming and higher SSTs. We interpret these trends to indicate the formation of a proto-warm pool at this time. The shoaling of the upper thermocline into the photic zone and the resulting enhanced productivity (relative to Interval 1) may have been facilitated by the creation of the EUC and its accompanying upward "expansion" of isotherms by analogy with the modern equatorial current system (Kennett et al., 1985; Hodell and Vayavananda, 1993; Stewart, 2005). The interval from ~11.7–11.2 Ma records the rapid warming of the deep thermocline based on sharply decreasing *Globoquadrina venezuelana* $\delta^{18}O$ values, with less pronounced warming of the upper thermocline based on decreasing *G. menardii* $\delta^{18}O$ values (Fig. 7). The interval from ~10.8–10.2 Ma records a second warming pulse of the deep and upper thermocline as seen in the parallel trends of *G. venezuelana* and *G. menardii*. In both cases, warming of the thermocline is associated with increased relative abundances of thermocline-

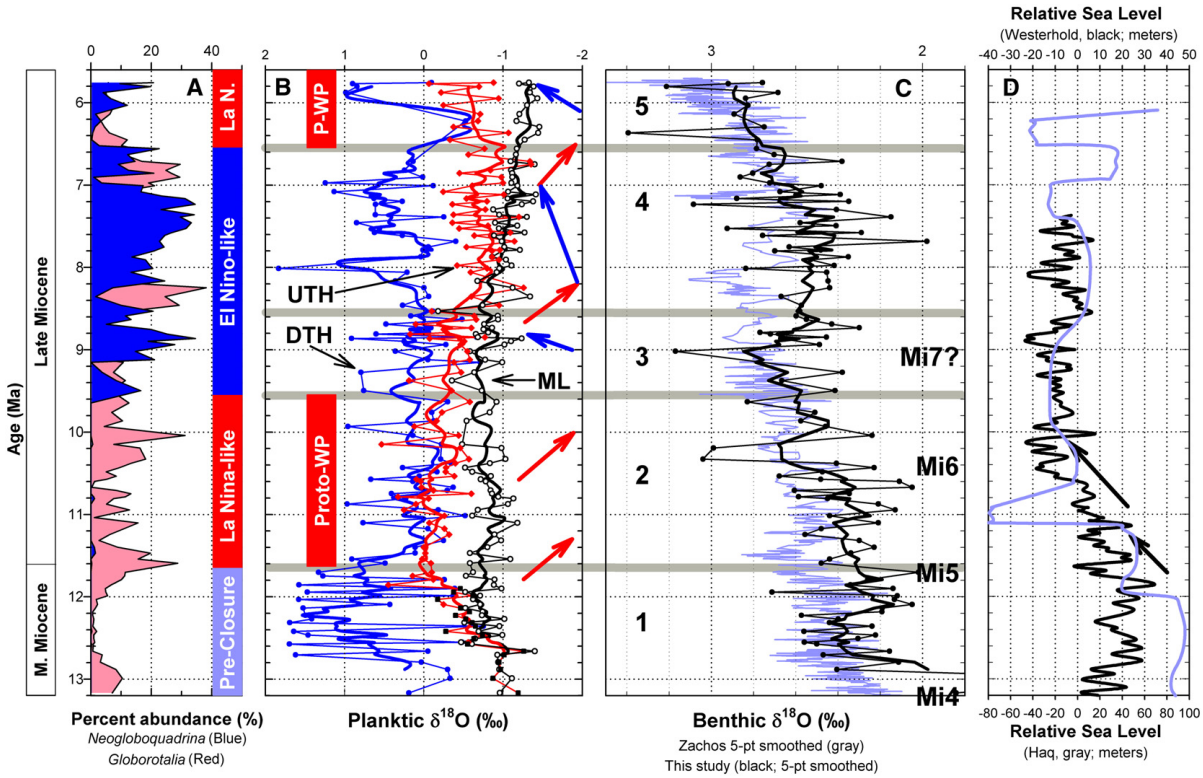

Fig. 7. Relative abundances of upper thermocline-dwelling *Globorotalia* spp. (red) and *Neogloboquadrina* spp. (blue) (panel A) are compared to an expanded multi-species planktic foraminiferal oxygen isotope record from Site 806 (panel B), benthic foraminiferal oxygen isotopes from Site 806 (black lines, including 5 pt. smoothed) and composite deep-sea record of Zachos et al., 2001 (panel C), and reconstructed sea level change of Westerhold et al., 2005 and Haq et al., 1987 (panel D). Note the correspondence between lower ('warming') $\delta^{18}O$ thermocline values (red arrows) and increased abundances of *Globorotalia* spp., and higher ('cooling') $\delta^{18}O$ thermocline values (blue arrows) and increased abundances of *Neogloboquadrina* spp. Also note correspondence between 'warming' thermocline and sea surface $\delta^{18}O$ values and falling sea level (Mi5, Mi6). (For interpretation of the references to color in this figure legend, the reader is referred to the web version of this article.)

dwelling species of *Globorotalia* (Fig. 7). In addition, the two-step warming of the thermocline precedes warming of the mixed layer suggesting that changes in the structure of the upper water column, perhaps including the development of the EUC, occurred before a measurable surface expression of the proto-warm pool.

The interpretation for the formation of a proto-warm pool and accompanying development of the EUC is supported by a large decrease in the upper water column oxygen isotope gradient between *G. venezuelana* and *G. sacculifer* ($\Delta\delta^{18}O_{DTH\text{-}ML}$), the convergence of $\delta^{18}O_{UTH}$ and $\delta^{18}O_{DTH}$ values, and by high abundances of mixed layer species, all of which typify a thick mixed layer and deep thermocline. Though the counts of thermocline species increased from Interval 1 to Interval 2, they are comparable to those seen in a modern box core sample from near the equator on Ontong Java Plateau (Table 2, Fig. 4E–G).Hodell and Vayavananda (1993, p. 304) predicted that the development of the Equatorial Undercurrent "should be evident by an increase in the abundance of intermediate-dwelling (i.e., upper thermocline) planktic foraminifers accompanied by a convergence in $\delta^{18}O$ values." This is precisely what we observed in the Site 806 time series, including an increase in thermocline species (*Globorotalia*) relative to Interval 1. By analogy with modern equatorial current processes (e.g., Stewart, 2005), the EUC could have the effect of doming cooler waters into the lower euphotic zone habitat of *G. menardii* during times of a proto-warm pool (Fig. 3). Because Site 806 was at or very near the Equator during late Miocene time, this process may explain why *G. menardii* and *G. sacculifer* oxygen isotope values diverged, while *G. venezuelana* and *G. sacculifer* values rapidly converged to create minimal deep thermocline-mixed layer oxygen isotope gradients. In other words, the deep thermocline warmed more than the upper thermocline, and sea surface temperatures warmed as well (Fig. 7).

Collectively, the foraminiferal census and isotope data suggest a two-stage intensification of a proto-warm pool during the early late Miocene. The coincidence with the Mi5 and Mi6 benthic oxygen isotope excursions is compelling. We suspect that warm pool development and intensification was facilitated by falling sea level at ~11.7–11.4 Ma, corresponding with oxygen isotope excursion Mi5, and again at ~10.6–10.4 Ma, corresponding with Mi6 (Wright et al., 1991; Miller et al., 1998; Turco et al., 2001; Billups and Schrag, 2002; Westerhold et al., 2005). This interval may include the largest sea level fall of the Miocene (Haq et al., 1987; Hardenbol et al., 1998; Isern et al., 2002). The question is whether the two-step development of a proto-warm pool was a culmination of Mi4 and Mi5 (50.0 +/− 5.0 m of sea level fall; John et al., 2004), or whether it was a culmination of Mi4, Mi5, and Mi6. The Mi5 and Mi6 benthic oxygen isotope excursions are weakly recorded in most deep-sea records (e.g., Zachos et al., 2001; Billups and Schrag, 2002). However, the Westerhold et al. (2005) isotope record from the South Atlantic suggests that Mi5 and Mi6 may in fact represent significant sea-level fall events of tens of meters each, and cumulatively ~50 m. In support of this interpretation, the Global boundary Stratotype Section and Point (GSSP) for the Serravalian–Tortonian stage boundary (middle–late Miocene boundary) is defined by a major sea-level fall event (Mi5) at 11.608 Ma (Hilgen et al., 2005). Further, John et al. (2006) documented pulses of increased kaolinite accumulation on the Marion Plateau (northeast Australian margin) during the middle Miocene and earliest late Miocene, which they attribute to reworking of early Miocene kaolinite-rich lacustrine deposits during lowstands, with peak kaolinite mass accumulation rates between 11 Ma and 10 Ma. This finding agrees well with the results of Ehrenberg et al. (2006) who used strontium-isotope stratigraphy to date the termination of the Northern Marion Plateau at ~10.7 Ma, which they attribute to a major sea-level lowstand (Mi6). This latter lowstand also correlates with a major sequence boundary on the Queensland Plateau (Betzler et al., 2000). A major flooding event at the base of the Tortonian stage (earliest late Miocene) may separate the Mi5 and Mi6 sea-level fall events as documented by Tcherepanov et al. (2008).

Hodell and Vayavananda (19993, p. 307) speculated about the significance of a sea level fall in reducing Indo-Pacific water exchange and giving rise to "essentially modern" tropical circulation patterns. The Mi5 and Mi6 events coincide with: 1) planktic foraminiferal population changes at Site 806 (Fig. 5), 2) warming of both the thermocline and sea surface temperatures in the WEP (Fig. 7), and 3) elevated rates of evolutionary turnover of thermocline dwelling planktic foraminifers (Fig. 6). Here, we hypothesize that sea level lowstands influenced Indonesian Throughflow, which in turn affected upper water column structure, equatorial circulation, and tropical planktic foraminifer evolution as a proto-warm pool developed in the WEP for the first time.

6.4. Onset of the "biogenic bloom" in the WEP (Interval 3: 9.6–8.6 Ma)

After ~9.6 Ma, the proto-warm pool waned, although the deterioration of the proto-warm pool is transitional over the 10.1 Ma to 9.2 Ma interval. This is best documented by 1) major changes in planktonic foraminiferal assemblages, including the decrease in mixed layer *Globigerinita glutinata* and rise in thermocline-dwelling *Neogloboquadrina* (Fig. 5), 2) the increase in the upper water column oxygen isotope gradient between *G. venezuelana* and *G. sacculifer* ($\Delta\delta^{18}O_{DTH\text{-}ML}$), and 3) more positive (cooler?) mixed layer ($\delta^{18}O_{ML}$) values (Fig. 6). Many sea-level curves depict a rise in sea-level after 9 Ma (Haq et al., 1987; Hardenbol et al., 1998; Westerhold et al., 2005). We can only speculate that this situation may have caused increased circulation through the Indonesian Seaway at this time resulting in the weakening of the proto-warm pool. Radiolarian abundances increase from <2% of the >63 μm fraction to >5% after 10.1 Ma (Fig. 4F). In addition, the biserial planktic foraminifer genus *Streptochilus*, known to be associated with productivity and oxygen minima, becomes persistent in the assemblages after ~10.1 Ma and then becomes persistently common after ~9.2 Ma at Site 806 with peak abundances of 39–48% in the >63 μm fraction during the interval from 8.9 Ma to 8.7 Ma (Resig, 1993). The increased abundances of *Streptochilus* and radiolarians suggest higher productivity. Planktic foraminiferal $\delta^{13}C$ values converge, reaching a minimum $\Delta\delta^{13}C_{ML\text{-}UTH}$ gradient ~9.0–8.8 Ma, further indicating increased productivity at this time (Fig. 4C and D). At nearby DSDP Site 289, Woodruff and Douglas (1981) note a significant decrease in the benthic foraminifer *Cibicidoides* and a large increase in *Uvigerina* ~9 Ma, which they attribute to increased productivity in the surface waters of the WEP.

The observed changes in planktic and benthic foraminiferal assemblages and isotope gradients coincide with the near collapse of the widespread calcareous nannofossil genus *Reticulofenestra* ~9.0–8.8 Ma at Site 806 (Takayama, 1993)(Fig. 4G). A similar collapse of large *Reticulofenestra* is observed in the Indian Ocean and Caribbean Sea, with the recovery of this genus being dominated by small forms (Young, 1990; Takayama, 1993; Kameo and Bralower, 2000). These dramatic changes in *Reticulofenestra* abundances at Site 806 and elsewhere imply the occurrence of an unidentified paleoceanographic event that may have been of a broad and unifying nature. One hypothesis is that this represents the onset of the widespread and long-lived "biogenic bloom" based on the abrupt increase in carbonate MARs at Site 806 (Fig. 8). This interval also coincides with a sharp increase in phosphorous MARs in the Indian Ocean (Hermoyian and Owen, 2001). Planktic foraminifers record significant assemblage changes, including an increase in *Neogloboquadrina acostaensis*, which may signal higher productivity, as well as a short-lived abundance spike of *Globoturborotalita nepenthes* that coincides with the climax of the *Reticulofenestra* event, peak *Streptochilus* abundances, and cooling thermocline temperatures (Figs. 5 and 7).

6.5. Absence of a proto-warm pool (Interval 4: 8.6–6.5 Ma)

The thermocline cooled at Ontong Java Plateau during this interval. There is a sharp increase in planktic foraminiferal diversity at ~8.6 Ma, which remains stable throughout this interval (Chaisson and Leckie, 1993;

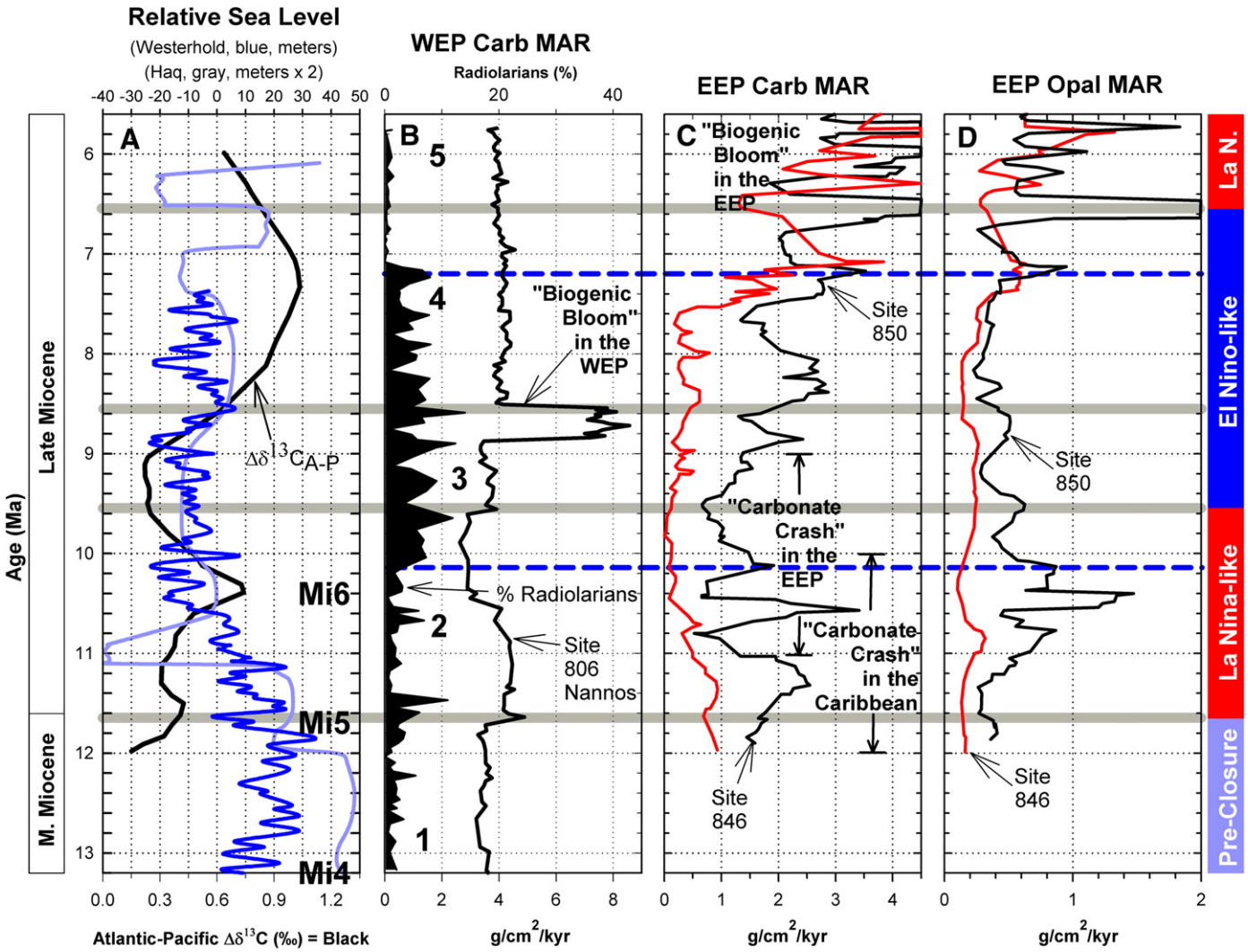

Fig. 8. Global seal level and deep-water circulation (panel A) compared with and biological productivity across the tropical Pacific Ocean (panels B–D). Panel A) Sea level based on Westerhold et al. (2005) and Haq et al. (1987). Mi4–Mi6 (Miocene isotope events) based on Wright et al. (1992) and Miller et al. (1998). Deep-water Atlantic–Pacific carbon isotope gradient from Lear et al. (2003). Panel B) WEP $CaCO_3$ MAR = Western Equatorial Pacific carbonate mass accumulation rate based on dry bulk density and percent carbonate values from Berger et al., 1991, and calcareous microfossil datums shown in Table 1. Percent radiolarians relative to total foraminifers picked from Site 806. "Biogenic bloom" in the WEP corresponds to marked increase in carbonate MARs and biotic changes associated with the 9.0–8.8 Ma interval discussed in text. Panel C) EEP $CaCO_3$ MAR = Eastern Equatorial Pacific carbonate mass accumulation rates for ODP Sites 846 and 850 (Farrell et al., 1995b). Panel D) EEP Opal MAR = Eastern Equatorial Pacific opal/silica mass accumulation rate s for ODP Sites 846 and 850 (Farrell et al., 1995b). "Biogeneic bloom" in the EEP from Farrell et al. (1995b) and Lyle et al. (1995). Duration of the "carbonate crash" in the Caribbean from Sigurdsson et al. (1997) and Roth et al. (2000)), and in the eastern equatorial Pacific from (Farrell et al., 1995b)). The dashed blue lines highlight the alternation of silica deposition from the EEP to the WEP and then back to the EEP during late Miocene time. (For interpretation of the references to color in this figure legend, the reader is referred to the web version of this article.)

Fig. 6). A broad increase in thermocline species abundances (averaging >30% of the assemblages, (Fig. 4E) and high $\Delta\delta^{18}O_{DTH\text{-}ML}$ gradients (Fig. 6) indicate non-warm pool conditions. This interval is characterized by an increase in the relative abundance of *Neogloboquadrina*, a tropical genus indicative of seasonal productivity (Fig. 5). This interpretation is further supported by the reduced $\delta^{13}C_{UTH\text{-}ML}$ gradient (Fig. 4D). We suggest that these biotic and physical changes in the upper water column indicate moderate (seasonal?) productivity; increased seasonality in the WEP may also explain why we see greater plantic foraminiferal diversity in this interval. This interval records the WEP continuation of the pan-tropical "biogenic bloom" (Peterson et al., 1992; Berger et al., 1993; Farrell et al., 1995b; Dickens and Owen, 1999; Grant and Dickens, 2002; Lyle, 2003). Kameo and Sato (2000) document a reconnection of Caribbean–eastern equatorial Pacific circulation at this time based on calcareous nannofossil assemblages.

Conditions began to change again in the WEP after ~7.2 Ma. Radiolarian abundances declined, and the thermocline warmed as evidenced by the declining oxygen isotope values of *G. venezuelana*. Changes in the dominant thermocline species of planktic foraminifera parallel the changes in the position and temperature of the upper thermocline as *Neogloboquadrina* decreased in relative abundance and *Globorotalia* increased. Collectively, these observations suggest that productivity declined in the WEP after ~7.2 Ma (Figs. 6 and 8).

6.6. Brief return of a proto-warm pool (Interval 5: 6.5–6.1 Ma)

After 6.5 Ma, there may have been a brief redevelopment of a proto-warm pool in the WEP based on the sharp decline in thermocline species abundance and abrupt warming of the deep thermocline as suggested by the rapid depletion of *G. venezuelana* oxygen isotope values ($\delta^{18}O_{DTH}$) and the convergence with *G. menardii* values ($\delta^{18}O_{TH}$), similar to that of Interval 2 (Figs. 4E and 6). Also noteworthy is the large drop in species diversity at ~6.4 Ma at Site 806 (Fig. 6)(Chaisson and Leckie, 1993) suggesting another major change in productivity, seasonality, and/or upper water column structure. The evolutionary first occurrence of the modern WPWP taxon *Pulleniatina* may reflect the reestablishment of a

proto-warm pool conditions in the WEP near the end of the Miocene (Figs. 5 and 6).

There is a question of whether the observed changes in WEP hydrography were triggered by falling sea level near the end of the Miocene similar to that of Interval 2 (Hodell et al., 1986; Kastens, 1992; Aharon et al., 1993; Hodell et al., 1994; Warny et al., 2003). Sea-level reconstructions show significant variability at this time with a major sea-level fall ~6.5 Ma (Haq et al., 1987; Hardenbol et al., 1998)(Fig. 8). After 6.1 Ma, thermocline taxa increase in abundance as the thermocline once again cools and shoals signaling the demise of proto-warm pool conditions.

7. Broader implications

We hypothesize that the initial development of a proto-warm pool in the WEP and its subsequent waxing and waning over time, contributed to El Niño-like and La Niña-like alternations in the structure of the upper water column across the equatorial Pacific. These changes influenced carbonate productivity and preservation (Fig. 8). We refer to these long-term changes in upper water column structure as "El Niño-like" and "La Niña-like" because they resemble the see-saw-like alternations of the thermocline profile represented by modern inter-annual ocean–climate variability of the equatorial Pacific (e.g., Ravelo et al., 2006).

This hypothesis may help to reconcile the long-standing mystery of why a "crash" in carbonate deposition in the Caribbean was not simultaneous with a very similar crash in the EEP (e.g., Farrell et al., 1995b; Sigurdsson et al., 1997; Roth et al., 2000). These changes in equatorial circulation and productivity may also lead to a better understanding of the variable character, timing, and magnitude of the pan-tropical "biogenic bloom".

In a general way, late Miocene productivity changes were antithetical between the WEP and EEP (Fig. 8). Productivity was suppressed in the WEP when a proto-warm pool developed ~12–10 Ma. The thermocline deepened in the west and shoaled in the east, and the EUC delivered nutrients eastward where it fed high productivity in the EEP. This scenario represents La Niña-like conditions across the equatorial Pacific. Conversely, when the proto-warm pool was weak or non-existent, especially ~9–7 Ma, productivity was relatively elevated in the WEP and suppressed in the EEP analogous to El Niño-like conditions today (Fig. 9).

Proto-warm pool development in the WEP coincided with the onset of the "carbonate crash" in the Caribbean based on the LO datum of *Globorotalia (Fohsella) fohsi* (11.68 Ma) at ODP Site 806 (Chaisson and Leckie, 1993) and ODP Site 999 in the Caribbean (Chaisson and D'Hondt, 2000). These two events also occurred when the Atlantic–Pacific carbon isotope gradient (i.e., NCW production) intensified in two steps approximately coincident with Miocene isotope events Mi5 and Mi6 at 11.7–11.5 Ma and 10.6–10.4 Ma, respectively (Fig. 8) (Flower and Kennett, 1993, 1994; Lear et al., 2003). These episodes of NCW production have been linked to the Caribbean "carbonate crash" by the concomitant influx of corrosive Antarctic Intermediate Water into the Caribbean due to the constriction of the Central American Seaway (Roth et al., 2000), or alternatively by the

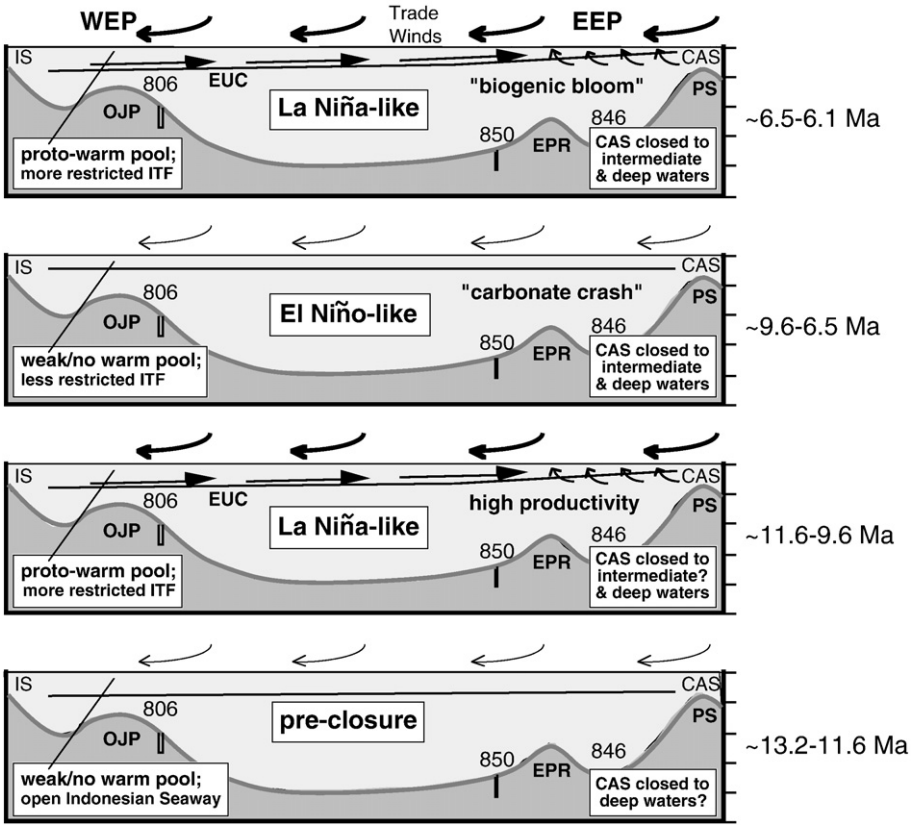

Fig. 9. Schematic representation of changing hydrography of the equatorial Pacific during the late middle and late Miocene affecting surface circulation, water column structure, and productivity. IS = Indonesian Seaway; ITF = Indonesian Throughflow; OJP = Ontong Java Plateau; EPR = East Pacific Rise; PS = Panama Sill; CAS = Central American Seaway; and 806 = ODP Site 806. Tick marks represent water depth in km. Panel A) ~13.2–11.6 Ma, pre-closure middle Miocene, trans-equatorial Pacific planktic foraminiferal assemblages are uniformly dominated by mixed layer species, thermocline species are scarce; represents a time when the IS and the CAS are open to intermediate water masses and the modern Pacific circulation pattern has not yet developed. Panel B) ~11.6–9.6 Ma, the early development of a proto-warm pool in the western equatorial Pacific (WEP), ITF has become restricted and modern Pacific circulation has begun, La Nina-like state; Equatorial Undercurrent (EUC) initiated and high productivity in the eastern equatorial Pacific (EEP), which effectively delayed the onset of the "carbonate crash" relative to the Caribbean basin, despite greater influx of corrosive, nutrient-rich deep waters into the Pacific. Panel C) ~9.6–6.5 Ma, proto-warm pool decay, increased productivity in the WEP (initial phase of "biogenic bloom") and decreased productivity in the EEP due to El Niño-like conditions resulting in intensification of the "carbonate crash" in the EEP. Panel D) Proto-warm pool resurgence ~6.5–6.1 Ma; re-established La Niña-like conditions with low productivity in the WEP and high productivity in the EEP and a strong "biogenic bloom".

influx of corrosive Pacific Intermediate Water (Newkirk and Martin, 2009). The Central American Seaway was becoming increasingly constricted at this time due to the uplift of the Central American volcanic arc and collision with the northwestern corner of South America (Duque-Caro, 1990; Coates et al., 2004). Lowering of sea-level during Mi5 may have contributed to changing source input to the Caribbean as suggested by the Neodymium isotopic data of Newkirk and Martin (2009). Continued emergence of the Isthmus of Panama and further reduction in Pacific–Caribbean exchange by ~10.7 Ma, roughly coincident with Mi6, is supported by Nd data (Newkirk and Martin, 2009), and by changes in calcareous nannofossil (Kameo and Sato, 2000) and planktic foraminifer assemblages (Chaisson and D'Hondt). Carbonate accumulation in the Caribbean recovered after ~10 Ma; a time coincident with the demise of the proto-warm pool in the WEP and decline of NCW production in the North Atlantic.

We hypothesize that the nearly 1 Myr offset in the initiation of the carbonate crash in the Caribbean and EEP was due to the establishment of La Niña-like conditions in the equatorial Pacific. La Niña-like conditions are a manifestation of increasingly constricted Indonesian Throughflow resulting in the deepening of the thermocline in the WEP (proto-warm pool) and strengthening of the EUC, which in turn sustained upwelling and carbonate productivity in the EEP. This heightened productivity effectively delayed the onset of the "carbonate crash" in the EEP (~11–9 Ma) relative to the Caribbean (~12–10 Ma), thereby dampening the effect of older, more corrosive deep waters that had begun to infiltrate the deep Pacific with increasing production of NCW after 12 Ma (Figs. 8 and 9).

From ~9.6 to 6.5 Ma, the proto-warm pool waned and El Niño-like conditions developed across the equatorial Pacific (Fig. 9). As a consequence, productivity increased in the WEP, particularly in the interval ~9.0–8.8 Ma. In the EEP, carbonate and siliceous productivity weakened as the EUC waned, warmer surface waters created a lid (Chavez et al., 1999), and the "carbonate crash" reached a nadir at ~9.5 Ma (Fig. 8) (Farrell et al., 1995b; Lyle et al., 1995; Cortese et al., 2004).

The redevelopment of a proto-warm pool in the WEP after ~6.5 Ma marks the return of La Niña-like conditions across the equatorial Pacific. However, unlike the 11.6–9.6 Ma interval, it is unclear whether falling sea level was a major contributor to increased constriction of ITF (e.g., Hodell et al., 2001; Warny et al., 2003). There was a rapid increase of carbonate and opal MARs at ODP Sites 846 and 850 in the EEP after 6.7 Ma (Farrell et al., 1995b; Lyle, 2003; Cortese et al., 2004). Reestablishment of the proto-warm pool and EUC may have facilitated higher productivity in the EEP. Kemp et al. (1995) documented two intervals of diatom mat deposition in the EEP: 14.6–9.5 Ma, and 6.3–6.1 Ma. The latter is the most intense period of mat deposition, which marks a second, stronger phase of the "biogenic bloom" in the EEP (Figs. 8 and 9).

8. Conclusions

Planktic foraminiferal census data, combined with oxygen and carbon isotopic data from three species of planktic foraminifer representing the mixed layer (*Globigerinoides sacculifer*), upper thermocline (*Globorotalia menardii*), and deep thermocline (*Globoquadrina venezuelana*), provide a robust record of changing upper water column conditions in the western equatorial Pacific for the interval 13.2–5.8 Ma. Changing oxygen isotopic gradients between the mixed layer and deep thermocline species ($\Delta\delta^{18}O_{DTH\text{-}ML}$) are a valuable proxy for the depth of the thermocline/thickness of the mixed layer; reduced gradients correspond with a deep thermocline, while expanded gradients correspond with a shallower thermocline. Changing oxygen isotopic gradients between the mixed layer and upper thermocline species ($\Delta\delta^{18}O_{UTH\text{-}ML}$) delimit warming and cooling trends in the upper thermocline, which are tracked by changes in the relative abundances of *Globorotalia* spp. and *Neogloboquadrina* spp., respectively. Changing carbon isotopic gradients between the mixed layer and upper thermocline species ($\Delta\delta^{13}C_{ML\text{-}UTH}$) after 9.2 Ma show variable, but higher levels of productivity in the western equatorial Pacific, which is also tracked by changes in the relative abundances of *Neogloboquadrina*. These proxy records suggest development of a proto-warm pool twice during the late Miocene as summarized below.

A trans-equatorial Pacific circulation existed until ~12 Ma (Kennett et al., 1985). This pre-closure tropical circulation represents a time when both the Indonesian and Central American seaways were becoming increasingly constricted but still open to intermediate water masses. The tectonic constriction of both seaways and a succession of sea level falls (Mi4, Mi5, and Mi6 events) may have reached a critical threshold after ~12 Ma, resulting in the restriction of Indonesian Throughflow and the formation of a more modern surface circulation system in the equatorial Pacific (Fig. 9).

A proto-warm pool developed and intensified in two stages coincident with the Mi5 isotope event (~11.7–11.6 Ma) and the Mi6 event (~10.6–10.4 Ma)(Westerhold et al., 2005), when sea level fell an estimated 50.0 +/− 5.0 m (Isern et al., 2002; John et al., 2004; Westerhold et al., 2005)(Fig. 6). We hypothesize that the production of Northern Component Water (NCW) was also modulated by the same cumulative effect of falling sea level in the early late Miocene (Fig. 8). The onset of the "carbonate crash", first in the Caribbean (~12–10 Ma) and later in the eastern equatorial Pacific (EEP; ~11–9 Ma) was due to the influx of corrosive intermediate waters into the Caribbean and relatively old, nutrient-rich deep waters into the Pacific as a consequence of increased NCW production coincident with the Mi5 and Mi6 isotope events. Development of a proto-warm pool initiated La Niña-like conditions and an Equatorial Undercurrent (EUC) that delivered nutrients to the central and eastern equatorial Pacific. This sustained productivity and effectively delayed the onset of the "carbonate crash" in the EEP relative to the Caribbean (Fig. 9).

As the proto-warm pool waned after 10 Ma, the EUC diminished and productivity decreased in the EEP. Onset of El Niño-like conditions resulted in moderate productivity and a weak or non-existent warm pool in the WEP ~9.6–6.5 Ma. Abrupt and widespread changes in calcareous nannofossil assemblages ~9.0–8.8 Ma mark the onset of the long-lived and variable "biogenic bloom" in the WEP (Fig. 8). Redevelopment of a short-lived proto-warm pool ~6.5–6.1 Ma caused a reduction in productivity in the WEP and La Niña-like conditions across the tropical Pacific that may have facilitated the strong late phase "biogenic bloom" in the EEP (Figs. 8 and 9).

Acknowledgements

We gratefully acknowledge support from the National Science Foundation OCE grant #0233992. Steve Nathan would also like to acknowledge the Geological Society of America Graduate Student Research Grant Program. The authors thank Steve Burns, Rob DeConto, Ben Flower and Dick Poore for their helpful advice. This manuscript greatly benefited from reviews of earlier drafts by Jerry Dickens, Cedric John, and Larry Peterson. We also thank Palaeo3 editor Thierry Corrège, and reviewers Ignacio Martinez and Kuo-Yen Wei for their valuable insights and suggestions. Gratitude is expressed to Ben Flower and Terry Quinn at the University of South Florida and to Dorinda Ostermann and Martha Jeglinski of Woods Hole Oceanographic Institution for use of their stable isotope mass spectrometer facilities. We would also like to thank Terry Quinn for producing preliminary Mg/Ca data from ODP Site 806. The authors also thank Bill Chaisson and the Ocean Drilling Program for samples.

Appendix A. Supplementary data

Supplementary data associated with this article can be found, in the online version, at doi:10.1016/j.palaeo.2009.01.007.

References

Acton, G.D., 1999. Apparent polar wander of India since the Cretaceous with implications for regional tectonics and true polar wander. In: Radhakrishna, T., Piper, J.D.A. (Eds.), The Indian Subcontinent and Gondwana: A Paleomagnetic and Rock Magnetic Perspective. Geological Society of India, Memoir, 44, pp. 129–175.

Aharon, P., Goldstein, S.L., Wheeler, C.W., Jacobson, G., 1993. Sea-level events in the South Pacific linked with the Messinian salinity crisis. Geology 21, 771–775.

Backman, J., Raffi, I., 1997. Calibration of Miocene nannofossil events to orbitally-tuned cyclostratigraphies from Ceara Rise. In: Shackleton, N.J., Curry, W.B., Richter, C., Bralower, T.J. (Eds.), Proceedings of the Ocean Drilling Program. Scientific Results, vol. 154. Ocean Drilling Program, College Station, TX, pp. 83–99.

Barrera, E., Keller, G., Savin, S.M., 1985. Evolution of the Miocene Ocean in the eastern North Pacific as inferred from oxygen and carbon isotope ratios of planktonic foraminifera. In: Kennett, J.P. (Ed.), The Miocene Ocean: Paleoceanography and Biogeography. Memoir, vol. 163. Geological Society of America, Boulder, CO, pp. 83–102.

Berger, W.H., Vincent, E., 1981. Chemostratigraphy and biostratigraphic correlation: exercises in systematic stratigraphy. Oceanolonogy Acta 4, 115–127 suppl.

Berger, W.H., Killingley, J.S., Vincent, E., 1978. Stable isotopes in deep-sea carbonates: Box Core ERDC-92, west equatorial Pacific. Oceanol. Acta 1, 203–216.

Berger, W.H., Kroenke, L., Janecek, T.R., et al., 1991. Proceedings of the Ocean Drilling Program. Initial Reports, p. 130.

Berger, W.H., Leckie, R.M., Janecek, T.R., Stax, R., Takayama, T., 1993. Neogene carbonate sedimentation on Ontong Java Plateau: highlights and open questions. In: Berger, W., Kroenke, L., Mayer, L. (Eds.), Proceedings of the Ocean Drilling Program. Scientific Results, vol. 130. Ocean Drilling Program, College Station, TX, pp. 711–744.

Berggren, W.A., Hollister, C.D., 1977. Plate tectonics and paleocirculation — commotion in the ocean. Tectonophysics 11, 11–48.

Berggren, W.A., Kent, D.V., Van Couvering, J., 1985. The Neogene: Part 2. Neogene chronology and chronostratigraphy. In: Snelling, N.J. (Ed.), The Geochronology and the Geological Record. Memoir, vol. 10. Geological Society of London, pp. 211–260.

Berggren, W.A., Kent, D.V., Swisher III, C.C., Aubry, M.-P., 1995. A revised Cenozoic geochronology and chronostratigraphy. In: Berggren, W.A., Kent, D.V., Aubry, M.-P., Hardenbol, J. (Eds.), Geochronology, Time Scales and Global Stratigraphic Correlation. Special Publication, 54. Society of Economic Paleontologists and Mineralalogists, pp. 129–212.

Betzler, C., Kroon, D., Reijmer, J.J.G., 2000. Synchroneity of major late Neogene sea level fluctuations and paleoceanographically controlled changes as recorded by two carbonate platforms. Paleoceanography 15, 722–730.

Bickert, T., Haug, G.H., Tiedemann, R., 2004. Late Neogene benthic stable isotope record of Ocean Drilling Program Site 999: implications for Caribbean paleoceanography, organic carbon burial, and the Messinian salinity crisis. Paleoceanography 19. doi:10.1029/2002PA000799 11 pp.

Billups, K., Schrag, D.P., 2002. Paleotemperatures and ice volumes of the past 27 Myr revisited with paired Mg/Ca and $^{18}O/^{16}O$ measurements on benthic foraminifera. Paleoceanography 17, 3–1–3-11.

Broecker, W.S., 1991. The great ocean conveyor. Oceanography 4, 79–89.

Cane, M.A., Molnar, P., 2001. Closing of the Indonesian seaway as a precursor to east African aridification around 3–4 million years ago. Nature 411, 157–162.

Cannariato, K.G., Ravelo, A.C., 1997. Pliocene–Pleistocene evolution of eastern tropical Pacific surface water circulation and thermocline depth. Paleoceanography 12, 805–820.

Cerling, T.E., Harris, J.M., MacFadden, B.J., Leakey, M.G., Quade, J., Eisenmann, V., Ehleringer, J.R., 1997. Global vegetation change through the Miocene/Pliocene boundary. Nature 389, 153–158.

Chaisson, W.P., 1995. Planktonic foraminiferal assemblages and paleoceanographic change in the trans-tropical Pacific Ocean: A comparison of west (Leg 130) and east (Leg 138), latest Miocene to Pleistocene. In: Pisias, N.G., Mayer, L.A., Janecek, T.R., Palmer-Julson, A., van Andel, T.H. (Eds.), Proceedings of the Ocean Drilling Program. Scientific Results, vol. 138. Ocean Drilling Program, College Station, TX, pp. 555–597.

Chaisson, W.P., D'Hondt, S.L., 2000. Neogene planktonic foraminifer biostratigraphy at Site 999, western Caribbean Sea. In: Leckie, R.M., Sigurdsson, H., Acton, G.D., Draper, G. (Eds.), Proceedings of the Ocean Drilling Program. Scientific Results, vol. 165. Ocean Drilling Program, College Station, TX, pp. 19–56.

Chaisson, W.P., Leckie, R.M., 1993. High-resolution Neogene planktonic foraminifer biostratigraphy of Site 806, Ontong Java Plateau (western equatorial Pacific). In: Berger, W.H., Kroenke, L.W., Mayer, L.A. (Eds.), Proceedings of the Ocean Drilling Program. Scientific Results, vol. 130. Ocean Drilling Program, College Station, TX, pp. 137–178.

Chaisson, W.P., Pearson, P.N., 1997. Planktonic foraminifer biostratigraphy at Site 925: middle Miocene–Pleistocene. In: Shackleton, N.J., Curry, W.B., Richter, C., Bralower, T.J. (Eds.), Proceedings of the Ocean Drilling Program. Scientific Results, vol. 154. Ocean Drilling Program, College Station, TX, pp. 3–31.

Chaisson, W.P., Ravelo, A.C., 1997. Changes in upper water-column structure at Site 925, late Miocene–Pleistocene; planktonic foraminifer assemblages and isotopic evidence. In: Shackleton, N.J., Curry, W.B., Richter, C., Bralower, T.J. (Eds.), Proceedings of the Ocean Drilling Program. Scientific Results, vol. 154. Ocean Drilling Program, College Station, TX, pp. 255–268.

Chaisson, W.P., Ravelo, A.C., 2000. Pliocene development of the east–west hydrographic gradient in the equatorial Pacific. Paleoceanography 10, 497–505.

Chavez, F.P., Strutton, P.G., Friederich, G.E., Feely, R.A., Feldman, G.C., Foley, D.G., McPhaden, M.J., 1999. Biological and chemical response of the equatorial Pacific Ocean to the 1997–98 El Niño. Science 286, 2126–2131.

Coates, A.G., Collins, L.S., Aubry, M.-P., Berggren, W.A., 2004. The geology of the Darien, Panama, and the late Miocene–Pliocene collision of the Panama arc with northwestern South America. Geological Society of America Bulletin 116 (11/12), 1327–1344.

Corfield, R.M., Cartlidge, J.E., 1993. Oxygen and carbon isotope stratigraphy of the middle Miocene, Holes 805B and 806B. In: Berger, W., Kroenke, L., Mayer, L., et al. (Eds.), Proceedings of the Ocean Drilling Program. Scientific Results, vol. 130. Ocean Drilling Program, College Station, TX, pp. 307–322.

Cortese, G., Gersonde, R., Hillenbrand, C.-D., Kuhn, G., 2004. Opal sedimentation shifts in the World Ocean over the last 15 myr. Earth and Planetary Science Letters 224, 509–527.

Covey, C., Barron, E.J., 1988. The role of ocean heat transport in climatic change. Earth Science Reviews 24, 429–445.

Curry, W.B., Thunell, R.C., Honjo, S., 1983. Seasonal changes in the isotopic composition of planktonic foraminifera collected in Panama Basin sediment traps. Earth and Planetary Science Letters 64, 33–43.

Dekens, P.S., Lea, D.W., Pak, D.K., Spero, H.J., 2002. Core top calibration of Mg/Ca in tropical foraminifera: Refining paleotemperature estimation. Geochemistry, Geophysics, Geosystems 3, 1022. doi:10.1029/2001GC000200.

Dickens, G.R., Owen, R.M., 1999. The latest Miocene–early Pliocene biogenic bloom: a revised Indian Ocean perspective. Marine Geology 161, 75–91.

Diester-Haass, L., Billups, K., Emeis, K.C., 2005. In search of the late Miocene–early Pliocene "biogenic bloom" in the Atlantic Ocean (Ocean Drilling Program Sites 982, 925, and 1088). Paleoceanography 20. doi:10.1029/2005PA001139 13 pp.

Droxler, A., Burke, K., Cunningham, A., Hine, A., Rosencrantz, E., Duncan, D., Hallock, P., Robinson, E., 1998. Caribbean constraints on circulation between Atlantic and Pacific oceans over the past 40 million years. In: Crowley, T., Burke, K. (Eds.), Tectonic boundary conditions for climate reconstructions. Oxford University Press, Oxford, pp. 169–191.

Duque-Caro, H., 1990. Neogene stratigraphy, paleoceanography and paleobiogeography in Northwest South America and the evolution of the Panama Seaway. Palaeogeography, Palaeoclimatology, Palaeoecology 77, 203–234.

Ehrenberg, S.N., McArthur, J.M., Thirlwall, M.F., 2006. Growth, demise, and dolomitization of Miocene carbonate platforms on the Marion Plateau, offshore NE Australia. Journal of Sedimentary Research 76, 91–116.

Fairbanks, R.G., Wiebe, P.H., 1980. Foraminifera and chlorophyll maximum: vertical distribution, seasonal succession, and paleoceanographic significance. Science 209, 1524–1526.

Fairbanks, R.G., Wiebe, P.H., Bé, A.W., 1980. Vertical distribution and isotopic composition of living planktonic foraminifera in the western North Atlantic. Science 207, 61–63.

Fairbanks, R.G., Sverdlove, M., Free, R., Wiebe, P.H., Bé, A.W., 1982. Vertical distribution and isotopic fractionation of living planktonic foraminifera from the Panama Basin. Nature 298, 841–844.

Farrell, J.W., Murray, D.W., McKenna, V.S., Ravelo, A.C., 1995a. Upper ocean temperature and nutrient contrasts inferred from Pleistocene planktonic foraminifer $\delta^{18}O$ and $\delta^{13}C$ in the eastern equatorial Pacific. In: Pisias, N.G., Mayer, L.A., Janecek, T.R., Palmer-Julson, A., van Andel, T.H. (Eds.), Proceedings of the Ocean Drilling Program. Scientific Results, vol. 138. Ocean Drilling Program, College Station, pp. 289–311.

Farrell, J.W., Raffi, I., Janecek, T., Murray, D.W., Levitan, M., Dadey, K.A., Emeis, K.C., Lyle, M., Flores, J.A., Hovan, S., 1995b. Late Neogene sedimentation patterns in the eastern Equatorial Pacific Ocean. In: Pisias, N.G., Mayer, L.A., Janecek, T.R., Palmer-Julson, A., van Andel, T.H. (Eds.), Proceedings of the Ocean Drilling Program. Scientific Results, vol. 138. Ocean Drilling Program, College Station, TX, pp. 717–756.

Faul, K.L., Ravelo, A.C., Delaney, M.L., 2000. Reconstructions of upwelling, productivity, and photic zone depth in the eastern equatorial Pacific Ocean using planktonic foraminiferal stable isotopes and abundances. Paleoceanography 30, 110–125.

Filippelli, G.M., 1997. Intensification of the Asian monsoon and a chemical weathering event in the late Miocene–early Pliocene: implications for late Neogene climate change. Geology 25, 27–30.

Filippelli, G.M., Delaney, M.L., 1994. The oceanic phosphorous cycle and continental weathering during the Neogene. Paleoceanography 9, 643–652.

Flower, B.P., Kennett, J.P., 1993. Middle Miocene ocean–climate transition; high-resolution oxygen and carbon isotopic records from Deep Sea Drilling Project Site 588A, southwest Pacific. Geology 21, 811–843.

Flower, B.P., Kennett, J.P., 1994. The middle Miocene climatic transition: East Antarctic ice sheet development, deep ocean circulation and global carbon cycling. Palaeogeography, Palaeoclimatology, Palaeoecology 108, 537–555.

Gasperi, J.T., Kennett, J.P., 1992. Isotopic evidence for depth stratification and paleoecology of Miocene planktonic foraminifera: western equatorial Pacific DSDP Site 289. In: Tsuchi, R., Ingle, J.C. (Eds.), Pacific Neogene — Environment, Evolution, and Events. University of Tokyo Press, pp. 117–147.

Gasperi, J.T., Kennett, J.P., 1993a. Miocene planktonic foraminifers at DSDP Site 289: depth stratification using isotopic differences. In: Berger, W., Kroenke, L., Mayer, L., et al. (Eds.), Proceedings of the Ocean Drilling Program. Scientific Results, vol. 130. Ocean Drilling Program, College Station, TX, pp. 323–332.

Gasperi, J.T., Kennett, J.P., 1993b. Vertical thermal structure evolution of Miocene surface waters: Western equatorial Pacific DSDP Site 289. Marine Micropaleontology 22, 235–254.

Goodman, P.J., Haxeleger, W., de Vries, P., Cane, M., 2005. Pathways into the Pacific Equatorial Undercurrent: a trajectory analysis. Journal of Physical Oceanography, 35, 2134–2151.

Gordon, A.L., 1986. Interocean exchange of thermocline water. Journal of Geophysical Research 91, 5037–5046.

Grant, K.M., Dickens, G.R., 2002. Coupled productivity and carbon isotope records in the southwest Pacific Ocean during the late Miocene–early Pliocene biogenic bloom. Palaeogeography, Palaeoclimatology, Palaeoecology 187, 61–82.

Haq, B.U., Hardenbol, J., Vail, P.R., 1987. Chronology of fluctuating sea levels since the Triassic (250 million years ago to present). Science 235, 1156–1167.

Hardenbol, J., Thierry, J., Farley, M.B., Jocquin, T., deGraciansky, P.-C., Vail, P.R., 1998. Mesozoic and Cenozoic sequence chronostratigraphic chart. In: deGraciansky, P.-C.,

Hardenbol, J., Jacquin, T., Vail, P.R. (Eds.), Mesozoic and Cenozoic Sequence Chronostratigraphic Framework of European Basins. Special Publication, vol. 60. Society of Sedimentary Geology (SEPM), pp. 3–13.
Haug, G.H., Tiedemann, R., 1998. Effect of the formation of the Isthmus of Panama on Atlantic Ocean thermohaline circulation. Nature 393, 673–676.
Heinze, C., Crowley, T.J., 1997. Sedimentary response to ocean gateway circulation changes. Paleoceanogrpahy 12, 742–754.
Hermoyian, C.S., Owen, R.M., 2001. Late Miocene–early Pliocene biogenic bloom: evidence from low-productivity regions of the Indian and Atlantic Oceans. Paleoceanography 16, 95–100.
Hilgen, F.J., Abdul Aziz, H., Bice, D., Iaccarino, S., Krijgsman, W., Kuiper, K., Montanari, A., Raffi, I., Turco, E., Zachariasse, W.J., 2005. The Global Boundary Stratotype Section and Point (GSSP) of the Tortonian stage (upper Miocene) at Monte dei Corvi. Episodes 28 (1), 6–17.
Hodell, D.A., Vayavananda, A., 1993. Middle Miocene paleoceanography of the western equatorial Pacific (DSDP Site 289) and the evolution of *Globorotalia* (*Fohsella*). Marine Micropaleontology 22, 279–310.
Hodell, D.A., Elmstrom, K.M., Kennett, J.P., 1986. Latest Miocene benthic $\delta^{18}O$ changes, global ice volume, sea level and the "Messinian salinity crisis". Nature 320, 411–414.
Hodell, D.A., Mueller, P.A., Garrido, J.R., 1991. Variations in the strontium isotopic composition of seawater during the Neogene. Geology 19, 24–27.
Hodell, D.A., Benson, R.H., Kent, D.V., Boersma, A., Rakic-El Bied, K., 1994. Magnetostratigraphic, biostratigraphic, and stable isotope stratigraphy of an upper Miocene drill core from the Sale Briqueterie (northwestern Morocco): a high-resolution chronology for the Messinian stage. Paleoceanography 9, 835–855.
Hodell, D.A., Curtis, J.H., Sierro, F.J., Raymo, M.E., 2001. Correlation of late Miocene to early Pliocene sequences between the Mediterranean and North Atlantic. Paleoceanography 16, 164–1783.
Isern, A.R., Anselmetti, F.S., Blum, P., et al., 2002. Proceedings of the Ocean Drilling Program. Initial Reports, vol. 194. Ocean Drilling Program, College Station, TX, pp. 1–88.
Jian, Z., Yu, Y., Li, B., Wang, J., Zhang, X., Zhou, Z., 2006. Phased evolution of the south–north hydrographic gradient in the South China Sea since the middle Miocene. Palaeogeography, Palaeoclimatology, Palaeoecology 230, 251–263.
Jiang, S., Wise Jr., S.W., Wang, J., 2007. Cause of the middle/late Miocene carbonate crash: Dissolution or low productivity? In: Teagle, D.A.H., Wilson, D.S., Acton, G.D., Vanko, D.A. (Eds.), Proceedings of the Ocean Drilling Program. Scientific Results, vol. 206. Ocean Drilling Program, College Station, TX.
John, C.M., Karner, G.D., Mutti, M., 2004. $\delta^{18}O$ and Marion Plateau backstripping: combining two approaches to constrain late middle Miocene eustatic amplitude. Geology 32, 829–832.
John, C.M., Adatte, T., Mutti, M., 2006. Regional trends in clay mineral fluxes to the Queensland margin and ties to middle Miocene global cooling. Palaeogeography, Palaeoclimatology, Palaeoecology 233, 204–224.
Kameo, K., Bralower, T.J., 2000. Neogene calcareous nannofossil biostratigraphy of Sites 998, 999, and 1000, Caribbean Sea. In: Leckie, R.M., Sigurdsson, H., Acton, G.D., Draper, G. (Eds.), Proceedings of the Ocean Drilling Program. Scientific Results, vol. 165. Ocean Drilling Program, College Station, TX, pp. 3–18.
Kameo, K., Sato, T., 2000. Biogeography of Neogene calcareous nannofossils in the Caribbean and the eastern equatorial Pacific — floral response to the emergence of the Isthmus of Panama. Marine Micropaleontology 39, 201–218.
Kastens, K.A., 1992. Did glacio-eustatic sea level drop trigger the Messinian salinity crisis? New evidence from Ocean Drilling Program Site 654 in the Tyrrhenian Sea. Paleoceanography 7, 333–356.
Keigwin, L.D., 1982. Isotope paleoceanography of the Caribbean and east Pacific: role of Panama uplift in late Neogene time. Science 217, 350–353.
Keller, G., 1985. Depth stratification of planktonic foraminifers in the Miocene ocean. In: Kennett, J.P. (Ed.), The Miocene Ocean: Paleoceanography and Biogeography, vol. 163. Geological Society of America Memoir, Boulder, CO, pp. 177–196.
Keller, G., Barron, J., 1983. Paleoceanographic implications of Miocene deep-sea hiatuses. Geological Society of America Bulletin 94, 590–613.
Kemp, A.E.S., Baldauf, J.G., Pearce, R.B., 1995. Origins and paleoceanographic significance of laminated diatom ooze from the eastern equatorial Pacific Ocean. In: Pisias, N.G., Mayer, L.A., Janecek, T.R., Palmer-Julson, A., van Andel, T.H. (Eds.), Proceedings of the Ocean Drilling Program. Scientific Results, vol. 138. Ocean Drilling Program, College Station, TX, pp. 641–645.
Kennett, J.P., 1977. Cenozoic evolution of Antarctic glaciation, the circum-Antarctic oceans and their impact on global paleoceanography. Journal of Geophysical Research 82, 3843–3859.
Kennett, J.P., Srinivasan, M.S., 1983. Neogene Planktonic Foraminifera. Hutchinson Ross Publ. Co., Stroudsburg.
Kennett, J.P., Keller, G., Srinivasan, M., 1985. Miocene planktic foraminifer biogeography and paleoceanographic development of the Indo-Pacific region. In: Kennett, J.P. (Ed.), The Miocene Ocean: Paleoceanography and Biogeography. Memoir, vol. 163. Geological Society of America, Boulder, CO, pp. 197–236.
Kroenke, L.W., Berger, W.H., Janecek, T.R., 1991. Proceedings of the Ocean Drilling Program. Initial Reports, vol. 130. Ocean Drilling Program, College Station, TX.
Kuhnt, W., Holbourn, A., Hall, R., Zuvela, M., Kaese, R., 2004. Neogene history of the Indonesian Throughflow. In: Continent-Ocean Interactions within East Asian Marginal Seas. AGU Geophysical Monograph Series 149, 299–320.
Lear, C.H., Rosenthal, Y., Wright, J.D., 2003. The closing of a seaway: ocean water masses and global climate change. Earth and Planetary Science Letters 210, 425–436.
Levitus, S., Boyer, T.P., 1994. World Ocean Atlas 1994. Temperature, NOAA Atlas NESDIS 4, vol. 4. U.S. Dept. of Commerce, Washington, D.C. 129 pp.
Levitus, S., Burgett, R., Boyer, T.P., 1994. World Ocean Atlas 1994. Salinity, NOAA Atlas NESDIS 3, vol. 3. U.S. Dept. of Commerce, Washington, D.C. 111 pp.
Li, Q., Li, B., Zhong, G., McGowran, B., Zhou, Z., Wang, J., Wang, P., 2006. Late Miocene development of the Western Pacific Warm Pool: Planktonic foraminifer and oxygen isotopic evidence. Palaeogeography, Palaeoclimatology, Palaeoecology 237, 465–482.
Loncaric, N., Peters, F.J.C., Kroon, K., Brummer, G.-J.A., 2006. Oxygen isotope ecology of recent planktic foraminifera at the central Walvis Ridge (SE Atlantic). Paleoceanography 21. doi:10.1029/2005PA001207.
Lyle, M., 2003. Neogene carbonate burial in the Pacific Ocean. Paleoceanography 18, 1–19.
Lyle, M., Dadey, K.A., Farrell, J.W., 1995. The late Miocene (11–8 Ma) eastern Pacific carbonate crash: evidence for reorganization of deep-water circulation by the closure of the Panama Gateway. In: Pisias, N.G., Mayer, L.A., Janecek, T.R., Palmer-Julson, A., van Andel, T.H. (Eds.), Proceedings of the Ocean Drilling Program. Scientific Results, vol. 138. Ocean Drilling Program, College Station, TX, pp. 821–838.
Martinez, J., Taylor, L., Deckker, P., Barrows, T., 1998. Planktonic foraminifera from the eastern Indian Ocean: distribution and ecology in relation to the Western Pacific Warm Pool (WPWP). Marine Micropaleontology 34, 121–151.
Martin, E.E., Shackleton, N.J., Zachos, J.C., Flower, B.P., 1999. Orbitally-tuned Sr isotope chemostratigraphy for the late middle to late Miocene. Paleoceanography 14, 74–83.
McPhaden, M., Picaut, J., 1990. El Niño-Southern Oscillation displacements of the western equatorial Pacific warm pool. Science 250, 1385–1388.
Mikolajewicz, U., Maier-Reimer, E., Crowley, T.J., Kim, K.-Y., 1993. Effect of Drake and Panamanian gateways on the circulation of an ocean model. Paleoceanography 8, 429–441.
Miller, K.G., Wright, J.D., Fairbanks, R.G., 1991. Unlocking the Ice House: Oligocene–Miocene oxygen isotopes, eustasy, and margina erosion. Journal of Geophysical Research 96, 6829–6848.
Miller, K.G., Mountain, G.S., Browning, J.V., Kominz, M., Sugerman, P.J., Christie-Blick, N., Katz, M., Wright, J.D., 1998. Cenozoic global sea level, sequences, and the New Jersey transect: results from coastal plain and continental slope drilling. Reviews of Geophysics 36, 569–601.
Molnar, P., Cane, M.A., 2002. El Niño's tropical climate and teleconnections as a blueprint for pre-ice age climates. Paleoceanography 17. doi:10.1029/2001PA000663.
Morey, S.L., Shriver, J.F., O'Brien, J.J., 1999. The effects of Halmahera on the Indonesian Throughflow. Journal of Geophysical Research 104 (C10), 23,281–23,296.
Nathan, S., 2005. Ontong Java Plateau and the South China Sea: Linkages to the Western Pacific Warm Pool, the East Asian Monsoon and Global Sea Level. Ph.D. dissertation, University of Massachusetts, Amherst.
Newkirk, D.R., Martin, E.E., 2009. Circulation through the Central American Seaway during the Miocene carbonate crash. Geology 37 (1), 87–90.
Nisancioglu, K.H., Raymo, M.E., Stone, P.H., 2003. Reorganization of Miocene deep water circulation in response to the shoaling of the Central American Seaway. Paleoceanography 18. doi:10.1029/2002PA000767.
Nishimura, S., Suparka, S., 1997. Tectonic approach to the Neogene evolution of Pacific–Indian Ocean seaways. Tectonophysics 281, 1–16.
Norris, R.D., Corfield, R.M., Cartlidge, J.E., 1993. Evolution of depth ecology in the planktic foraminifera lineage *Globorotalia* (*Fohsella*). Geology 21, 975–978.
Patrick, A., Thunell, R.C., 1997. Tropical Pacific sea surface temperatures and upper water column thermal structure during the last glacial maximum. Paleoceanography 12, 649–657.
Pearson, P.N., Shackleton, N.J., 1995. Neogene multispecies planktonic foraminifer stable isotope record, Site 871, Limalok Guyot. In: Haggerty, J.A., Premoli Silva, I., Rack, F., McNutt, M.K. (Eds.), Proceedings of the Ocean Drilling Program, Scientific Results, vol. 144. Ocean Drilling Program, College Station, TX, pp. 401–410.
Peterson, L.C., Murray, D.W., Ehrmann, W.U., Hempel, P., 1992. Cenozoic carbonate accumulation and compensation depth changes in the Indian Ocean. In: Duncan, R.A., Rea, D.K., Kidd, R.B., von Rad, U., Weissel, J.K. (Eds.), Synthesis of Results from Scientific Drilling in the Indian Ocean, vol. 70. AGU Geophysical Monograph, pp. 311–333.
Philander, S.G.H., 1980. The Equatorial Undercurrent revisited. Annual Reviews of Earth and Planetary Sciences 8, 191–204.
Pisias, N.G., Mayer, L.A., Mi, A., 1995. Paleoceanography of the eastern equatorial Pacific during the Neogene: synthesis of Leg 138 drilling results. In: Pisias, N.G., Mayer, L.A., Janecek, T.R., Palmer-Julson, A., van Andel, T.H. (Eds.), Proceedings of the Ocean Drilling Program. Scientific Results, vol. 138. Ocean Drilling Program, College Station, TX, pp. 5–21.
Raffi, I., Flores, J.-A., 1995. Pleistocene through Miocene calcareous nannofossils from eastern equatorial Pacific Ocean (Leg 138). In: Pisias, N.G., Mayer, L.A., Janecek, T.R., Palmer-Julson, A., van Andel, T.H. (Eds.), Proceedings of the Ocean Drilling Program. Scientific Results, vol. 138. Ocean Drilling Program, College Station, TX, pp. 233–286.
Raffi, I., Backman, J., Fornaciari, E., Palike, H., Rio, D., Lourens, L., Hilgen, F., 2006. A review of calcareous nannofossil astrobiochronology encompassing the past 25 million years. Quaternary Science Reviews. doi:10.1016/j.quascirev.2006.07.007.
Ravelo, A.C., Fairbanks, R.G., 1992. Oxygen isotopic composition of multiple species of planktonic foraminifera: recorders of the modern photic zone temperature gradient. Paleoceanography 7, 815–831.
Ravelo, A.C., Fairbanks, R.G., 1995. Carbon isotopic fractionation in multiple species of foraminifera from core-tops in the tropical Atlantic. Journal of Foraminiferal Research 25, 53–74.
Ravelo, A.C., Shackleton, N.J., 1995. Evidence for surface-water circulation changes at Site 851 in the eastern tropical Pacific Ocean. In: Pisias, N.G., Mayer, L.A., Janecek, T.R., Palmer-Julson, A., van Andel, T.H. (Eds.), Proceedings of the Ocean Drilling Program. Scientific Results, vol. 138. Ocean Drilling Program, College Station, TX, pp. 503–514.
Ravelo, A.C., Andreasen, D.H., Lyle, M., Lyle, A.O., Wara, M.W., 2004. Regional climate shifts caused by gradual cooling in the Pliocene epoch. Nature 429, 263–267.
Ravelo, A.C., Dekens, P.S., McCarthy, M., 2006. Evidence for El Niño-like conditions during the Pliocene. GSA Today 16, 4–11.
Raymo, M.E., 1994. The initiation of northern hemisphere glaciation. Annual Reviews of Earth and Planetary Science 22, 353–383.

Rea, D.K., 1992. Delivery of Himalayan sediment to the northern Indian Ocean and its relation to global climate, sea level, uplift and seawater strontium. In: Duncan, R.A., Rea, D.K., Kidd, R.B., von Rad, U., Weissel, J.K. (Eds.), Synthesis of Results from Scientific Drilling in the Indian Ocean, vol. 70. AGU Geophysical Monograph, pp. 382–402.

Resig, J.M., 1993. Cenozoic stratigraphy and paleoceanography of biserial planktonic foraminifers, Ontong Java Plateau. In: Berger, W.H., Kroenke, L.W., Mayer, L.A. (Eds.), Proceedings of the Ocean Drilling Program. Scientific Results, vol. 130. Ocean Drilling Program, College Station, TX, pp. 231–244.

Rodgers, K.B., Latif, M., Legutke, S., 2000. Sensitivity of equatorial Pacific and Indian Ocean watermasses to the position of the Indonesian Throughflow. Geophysical Research Letters 27 (18), 2914–2944.

Romine, K., Lombari, G., 1985. Evolution of Pacific circulation in the Miocene: radiolarian evidence from DSDP Site 289. In: Kennett, J.P. (Ed.), The Miocene Ocean: Paleoceanography and Biogeography, vol. 163. Geological Society of America Memoir, Boulder, CO, pp. 273–290.

Roth, J.M., Droxler, A.W., Kameo, K., 2000. The Caribbean carbonate crash at the middle to late Miocene transition: linkage to the establishment of the modern global ocean conveyor. In: Leckie, R.M., Sigurdsson, H., Acton, G.D., Draper, G. (Eds.), Proceedings of the Ocean Drilling Program. Scientific Results, vol. 165. Ocean Drilling Program, College Station, TX, pp. 249–273.

Sato, K., Oda, M., Chiyonobu, S., Kimoto, K., Domitsu, H., Ingle Jr., J.C., 2008. Establishment of the western Pacific warm pool during the Pliocene: evidence from planktic foraminifera, oxygen isotopes, and Mg/Ca ratios. Palaeogeography, Palaeoclimatology, Palaeoecology 265, 140–147.

Savin, S.M., Abel, L., Barrera, E., Hodell, D.A., Keller, G., Kennett, J.P., Murphy, M., Vincent, E., 1985. The evolution of Miocene surface and near-surface marine temperatures: oxygen isotopic evidence. In: Kennett, J.P. (Ed.), The Miocene Ocean: Paleoceanography and Biogeography, vol. 163. Geological Society of America Memoir, Boulder, CO, pp. 42–82.

Schneider, B., Schmittner, A., 2006. Simulating the impact of the Panamanian seaway closure on ocean circulation, marine productivity, and nutrient cycling. Earth and Planetary Science Letters 246, 367–380.

Shackleton, N.J., Crowhurst, S., Hagelberg, T., Pisias, N.G., Schneider, D.A., 1995. A new late Neogene time scale: application to Leg 138 sites. In: Pisias, N.G., Mayer, L.A., Janecek, T.R., Palmer-Julson, A., van Andel, T.H. (Eds.), Proceedings of the Ocean Drilling Program. Initial Reports, vol. 138, pp. 73–101.

Shriver, J.F., Hurlburt, H.E., 1997. The contribution of the global thermocline circulation to the Pacific to Indian Ocean throughflow via Indonesia. Journal of Geophysical Research 102 (C3), 5491–5511.

Sigurdsson, H., Leckie, R.M., Acton, G.D., 1997. Proceedings of the Ocean Drilling Program. Initial Reports, vol. 165. Ocean Drilling Program, College Station, TX.

Spencer-Cervato, C., 1998. Changing depth distribution of hiatuses during the Cenozoic. Paleoceanography 13, 178–182.

Srinivasan, M.S., Kennett, J.P., 1981. Neogene planktonic foraminiferal biostratigraphy and evolution: equatorial to subantarctic South Pacific. Marine Micropaleontology 6, 499–533.

Srinivasan, S., Sinha, R., 1998. Early Pliocene closing of the Indonesian Seaway: evidence from northeast Indian Ocean and Tropical Pacific deep sea cores. Journal of Asian Earth Sciences 16, 29–44.

Stewart, R.H., 2005. Introduction to Physical Oceanography. Department of Oceanography, Texas A and M University. Open source textbook, http://oceanworld.tamu.edu/resources/ocng_textbook/contents.html.

Takayama, T., 1993. Notes on Neogene calcareous nannofossil biostratigraphy of the Ontong Java Plateau and size variations of *Reticulofenestra* coccoliths. In: Berger, W.H., Kroenke, L.W., Mayer, L.A. (Eds.), Proceedings of the Ocean Drilling Program. Scientific Results, vol. 130. Ocean Drilling Program, College Station, TX, pp. 179–230.

Tcherepanov, E.N., Droxler, A.W., Lapointe, P., Mohn, K., 2008. Carbonate seismic stratigraphy of the Gulf of Papua mixed depositional system: Neogene stratigraphic signature and eustatic control. Basin Research 20, 185–209.

Theyer, F., Vincent, E., Mayer, L.A., 1989. Sedimentation and paleoceanography of the central equatorial Pacific. In: Winterer, E.L., Hussong, D.M., Decker, R.W. (Eds.), The Eastern Pacific Ocean and Hawaii. The Geology of North America N. Geological Society of America, pp. 347–372.

Thunell, R.C., Reynolds, L.A., 1984. Sedimentation of planktonic foraminifera: seasonal changes in species flux in the Panama Basin. Micropaleontology 30, 243–262.

Thunell, R.C., Curry, W.B., Honjo, S., 1983. Seasonal variation in the flux of planktonic foraminifera: time series sediment trap results from the Panama Basin. Earth and Planetary Science Letters 64, 44–55.

Tomczak, M., Godfrey, J.S., 1994. Regional Oceanography: An Introduction. Pergamon Press, Oxford, 442 p.

Turco, E., Hilgen, F.J., Lourens, L.J., Shackleton, N.J., Zachariasse, W.J., 2001. Punctuated evolution of global climate cooling during the late middle to early late Miocene: high-resolution planktonic foraminiferal and oxygen isotope records from the Mediterranean. Paleoceanography 16, 405–423.

van Andel, Tj.H., 1975. Mesozoic/Cenozoic calcite compensation depth and the global distribution of calcareous sediments. Earth and Planetary Science Letters 26, 187–194.

van Andel, Tj.H., Heath, G.R., Moore Jr., T.C., 1975. Cenozoic history and paleoceanography of the central equatorial Pacific Ocean. Geological Society of America Memoir 143 134 p.

Vincent, E., Berger, W.H., 1985. Carbon dioxide and polar cooling in the Miocene: the Monterey hypothesis. In: Sundquist, E.T., Broecker, W.S. (Eds.), The Carbon Cycle and Atmospheric CO_2: Natural Variations Archean to Present. American Geophsical Union, Washington, D.C., pp. 455–468.

Vincent, E., Killingley, J.S., 1985. Oxygen and carbon isotope record for the early and middle Miocene in the central equatorial Pacific, Leg 85, and paleoceanographic implications. In: Mayer, L.A., Theyer, F. (Eds.), Initial Reports of the Deep Sea Drilling Project, vol. 85, pp. 749–770.

Vincent, E., Toumarkine, M., 1995. Data Report: Miocene planktonic foraminifers from the eastern equatorial Pacific. In: Pisias, N.G., Mayer, L.A., Janecek, T.R., Palmer-Julson, A., van Andel, T.H. (Eds.), Proceedings of the Ocean Drilling Program. Initial Reports, vol. 138, pp. 895–907.

Vincent, E., Killingley, J.S., Berger, W., 1980. The magnetic epoch 6 carbon shift: a change in the ocean's $^{13}C/^{12}C$ ratio 6.2 million years ago. Marine Micropaleontology 5, 185–203.

Vincent, E., Killingley, J.S., Berger, W., 1981. Stable isotope composition of benthic foraminifera from the equatorial Pacific. Nature 289, 639–643.

Wan, S., Li, A., Clift, P.D., Jiang, H., 2006. Development of the East Asian summer monsoon: Evidence from the sediment record in the South China Sea since 8.5 Ma. Palaeogeography, Palaeoclimatology, Palaeoecology 241, 139–159.

Wara, M.W., Ravelo, A.C., Delaney, M.L., 2005. Permanent El Nino-like conditions during the Pliocene warm period. Science 309, 758–761.

Warny, S.A., Bart, P.J., Suc, J.-P., 2003. Timing and progression of climatic, tectonic and glacioeustatic influences on the Messinian Salinity Crisis. Palaeogeography, Palaeoclimatology, Palaeoecology 202, 59–66.

Webster, P.J., 1994. The role of hydrological processes in ocean–atmosphere interactions. Reviews of Geophysics 32, 427–476.

Wells, M.L., Vallis, G.K., Silver, E.A., 1999. Tectonic processes in Papua New Guinea and past productivity in the eastern equatorial Pacific Ocean. Nature 398, 601–604.

Westerhold, T., Bickert, T., Röhl, U., 2005. Middle to late Miocene oxygen isotope stratigraphy of ODP Site 1085 (SE Atlantic): new constraints on Miocene climate variability and sea-level fluctuations. Palaeogeography, Palaeoclimatology, Palaeoecology 217, 205–222.

Woodruff, F., Douglas, R.G., 1981. Response of deep-sea benthic foraminifera to Miocene paleoclimatic events, DSDP Site 289. Marine Micropaleontology 6, 617–632.

Wright, J.D., Miller, K.G., Fairbanks, R.G., 1991. Evolution of modern deepwater circulation: evidence from the late Miocene Southern Ocean. Paleoceanography 6, 275–290.

Wright, J.D., Miller, K.G., Fairbanks, R.G., 1992. Early and middle Miocene stable isotopes: implications for deepwater circulation and climate. Paleoceanography 7, 357–389.

Yamasaki, M., Sasaki, A., Oda, M., Domitsu, H., 2008. Western equatorial Pacific planktic foraminiferal fluxes and assemblages during a La Niña year (1999). Marine Micropaleontology 66, 304–319.

Yan, X., Ho, C., Zheng, Q., Klemas, V., 1992. Temperature and size variabilities of the Western Pacific Warm Pool. Science 258, 1643–1645.

Young, J., 1990. Size variation of Neogene *Reticulofenestra* coccoliths from Indian Ocean DSDP Cores. Journal of Micropaleontology 9, 71–96.

Zachos, J., Pagani, M., Sloan, L., Thomas, E., Billups, K., 2001. Trends, rhythms, and aberrations in global climate 65 Ma to present. Science 292, 686–693.

Ziegler, C.L., Murray, R.W., Hovan, S.A., Rea, D.K., 2007. Resolving eolian, volcanogenic, and authigenic components in pelagic sediment from the Pacific Ocean. Earth and Planetary Science Letters 254, 416–432.